

REPORT ON A HELICOPTER-BORNE Z-AXIS TIPPER ELECTROMAGNETIC (ZTEM) AND AEROMAGNETIC GEOPHYSICAL SURVEY

Gibraltar Mine (Clipped)
McLeese Lake, British Columbia

For:
Gibraltar Mines Ltd.

BC Geological Survey
Assessment Report
32225b

By:

Geotech Ltd.
245 Industrial Parkway North
Aurora, Ont., CANADA, L4G 4C4
Tel: 1.905.841.5004
Fax: 1.905.841.0611
www.geotech.ca
Email: info@geotech.ca



Survey flown on January 8th – January 24th 2011
Project 1010
March 2011

TABLE OF CONTENTS

| | |
|--|------------|
| EXECUTIVE SUMMARY | III |
| 1. INTRODUCTION..... | 1 |
| 1.1 General Considerations..... | 1 |
| 1.2 Survey Location..... | 2 |
| 1.3 Topographic Relief and Cultural Features | 3 |
| 2. DATA ACQUISITION..... | 4 |
| 2.1 Survey Area | 4 |
| 2.2 Survey Operations | 4 |
| 2.3 Flight Specifications..... | 5 |
| 2.4 Aircraft and Equipment..... | 5 |
| 2.4.1 Survey Aircraft | 5 |
| 2.4.2 Airborne Receiver..... | 5 |
| 2.4.3 Base Station Receiver..... | 6 |
| 2.4.4 Airborne magnetometer..... | 7 |
| 2.4.5 Radar Altimeter..... | 7 |
| 2.4.6 GPS Navigation System..... | 7 |
| 2.4.7 Digital Acquisition System..... | 8 |
| 2.4.8 Mag Base Station | 8 |
| 3. PERSONNEL..... | 9 |
| 4. DATA PROCESSING AND PRESENTATION | 10 |
| 4.1 Flight Path | 10 |
| 4.2 In-field Processing and Quality Control..... | 10 |
| 4.3 GPS Processing..... | 10 |
| 4.4 ZTEM Electromagnetic Data..... | 11 |
| 4.4.1 Preliminary Processing..... | 11 |
| 4.4.2 Geosoft Processing..... | 11 |
| 4.4.3 Final Processing | 12 |
| 4.4.4 ZTEM Profile Sign Convention | 12 |
| 4.4.5 ZTEM Quadrature Sign Dependence..... | 13 |
| 4.4.6 Total Divergence and Phase Rotation Processing | 14 |
| 4.5 Magnetic Data..... | 15 |
| 5. DELIVERABLES | 16 |
| 5.1 Survey Report..... | 16 |
| 5.2 Maps | 16 |
| 5.3 Digital Data..... | 16 |
| 6. CONCLUSIONS AND RECOMMENDATIONS | 20 |
| 6.1 Conclusions..... | 20 |
| 6.2 Recommendations | 20 |
| 7. REFERENCES AND SELECTED BIBLIOGRAPHY | 21 |

LIST OF FIGURES

| | |
|---|----|
| Figure 1 - Property Location..... | 1 |
| Figure 2 – The Clipped Block, with ZTEM and Magnetic Base Station Locations | 2 |
| Figure 3 – Google Earth image of the Block | 3 |
| Figure 4 - ZTEM System Configuration..... | 6 |
| Figure 5 - ZTEM base station receiver coils..... | 7 |
| Figure 6 - ZTEM Crossover Polarity Convention of the Block..... | 12 |
| Figure 7 - Illustration of ZTEM In-Phase & Quadrature Tipper transfer function polarity convention..... | 13 |

LIST OF TABLES

| | |
|--------------------------------------|---|
| Table 1 - Survey Specifications..... | 4 |
|--------------------------------------|---|

| | |
|--|----|
| Table 2 - Survey schedule..... | 4 |
| Table 3 - Acquisition and Processing Sampling Rates..... | 8 |
| Table 4 - Geosoft GDB Data Format..... | 17 |

APPENDICES

| | |
|---|--|
| A. Survey location maps..... | |
| B. Survey Block Coordinates..... | |
| C. Geophysical Maps | |
| D. ZTEM Theoretical Considerations | |
| E. ZTEM Tests over Unconformity Uranium Deposits..... | |

REPORT ON A HELICOPTER-BORNE Z-AXIS, TIPPER ELECTROMAGNETIC GEOPHYSICAL SURVEY

Gibraltar Mine (Clipped)
McLeese Lake, British Columbia

Executive Summary

During January 8th to January 24th 2011 Geotech Ltd. carried out a helicopter-borne geophysical survey for Gibraltar Mines Ltd. over the Gibraltar Mine Property situated 3 kilometres north of McLeese Lake, British Columbia, Canada. This area was requested to be clipped to the mineral property boundary.

Principal geophysical sensors included a Z-Axis Tipper electromagnetic (ZTEM) system, and a caesium magnetometer. Ancillary equipment included a GPS navigation system and a radar altimeter. A total of 756.3 line-kilometres of geophysical data were acquired during their survey. The total line-kilometres once clipped to the mineral property boundary was 560.1

The survey operations were based out of the town of Williams Lake, British Columbia. In-field data quality assurance and preliminary processing were carried out on a daily basis during the acquisition phase. Preliminary and final data processing, including generation of final digital data and map products were undertaken from the office of Geotech Ltd. in Aurora, Ontario.

The survey report describes the procedures for data acquisition, processing, final image presentation and the specifications for the digital data set. In addition, 2D Inversions have been provided in the report (Appendix F) in support of the data. Further analysis of this data is recommended in conjunction with the geology prior to drill testing.

1. INTRODUCTION

1.1 General Considerations

These services are the result of the Agreement made between Geotech Ltd. and Gibraltar Mines Ltd. to perform a helicopter-borne geophysical survey over the Gibraltar Mine Property located 3 kilometres north of McLeese Lake, British Columbia, Canada (Figure 1).

John Fleming represented Gibraltar Mines Ltd. during the data acquisition and data processing phases of this project.

The geophysical surveys consisted of helicopter borne AFMAG Z-axis Tipper electromagnetic (ZTEM) system and aero magnetics using a caesium magnetometer. A total of 560.1 line kilometres of geophysical data were acquired once the clip to the boundary was made. The survey area is shown in Figure 2.

In a ZTEM survey, a single vertical-dipole air-core receiver coil is flown over the survey area in a grid pattern, similar to regional airborne EM surveys. Two orthogonal, air-core horizontal axis coils are placed close to the survey site to measure the horizontal EM reference fields. Data from the three coils are used to obtain the Tzx and Tzy Tipper (Vozoff, 1972) components at five frequencies in the 30 to 360 Hz band. The ZTEM data provides useful information on geology using resistivity contrasts while magnetometer data provides additional information on geology using magnetic susceptibility contrasts.



Figure 1 -Property Location

The crew was based out of the Super 8 Hotel in Williams Lake, British Columbia for the acquisition phase of the survey. Survey flying was started on January 8th 2011 and finished on January 24th 2011.

Data quality control and quality assurance, and preliminary data processing were carried out on a daily basis during the acquisition phase of the project. Final reporting, data presentation and archiving were completed from the Aurora office of Geotech Ltd. in March 2011.

1.2 Survey Location

The Gibraltar Mine Property is located approximately 3 kilometres to the North of McLeese Lake, British Columbia, as shown in Figure 2.

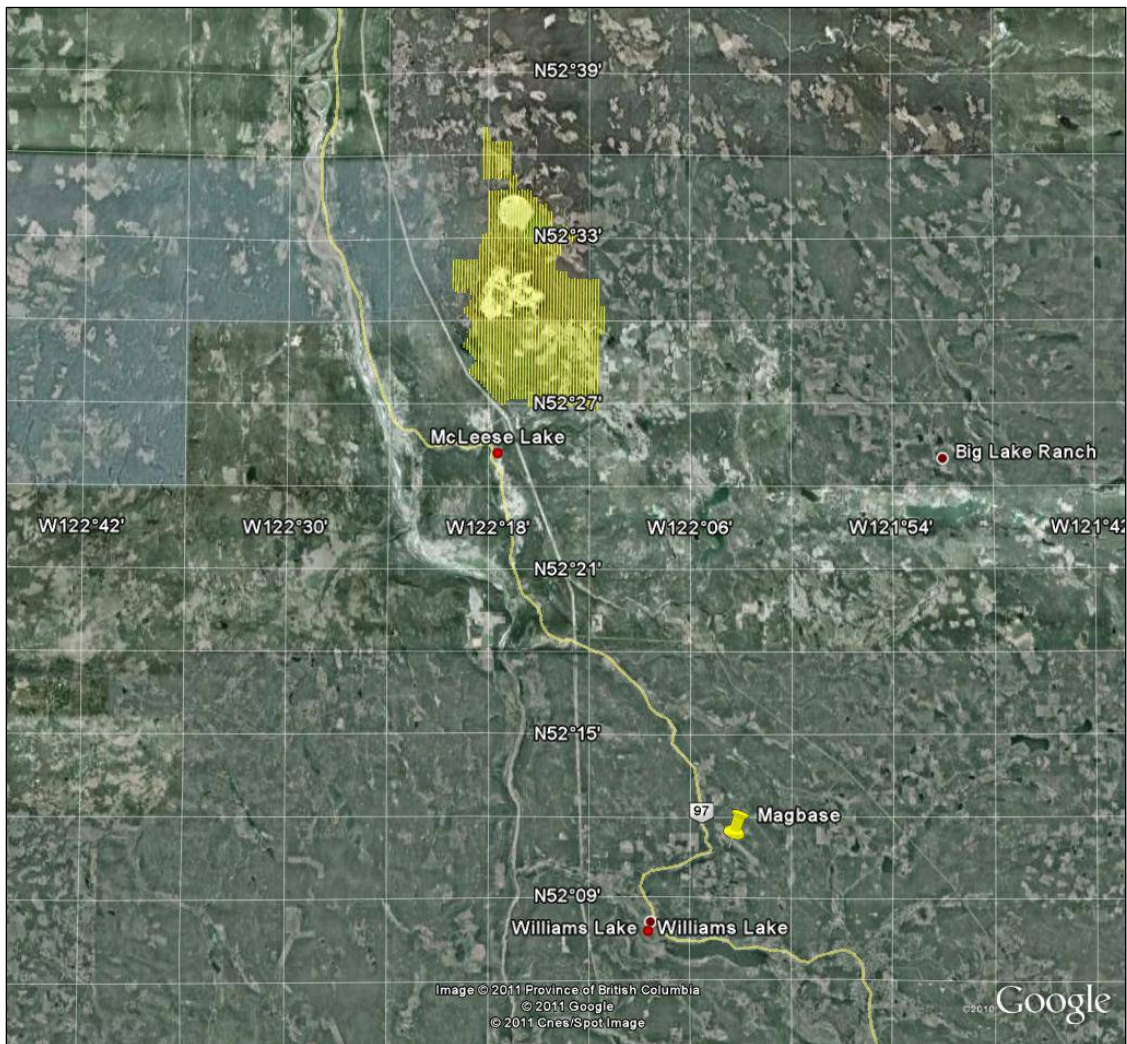


Figure 2 – The Survey Area with ZTEM and Magnetic Base Station Locations

It was flown in a North to South (N 0° E / N 180° E) direction, with a flight line spacing of 200 metres, as depicted in Figure 3. For more detailed information on the flight spacing and direction see Table 1.

1.3 Topographic Relief and Cultural Features

The Gibraltar Mine Property exhibits a moderate relief covering 111 square kilometres (see Figure 3). The survey area has various visible signs of culture such as, roads, transmission lines & buildings which are throughout the survey. There are also numerous river and streams which connect various lakes and wetlands. Special care is recommended in identifying any other potential cultural features from other sources that might be recorded in the data. The survey block covers a number of British Columbia Mining Claims, which are shown in Appendix A.

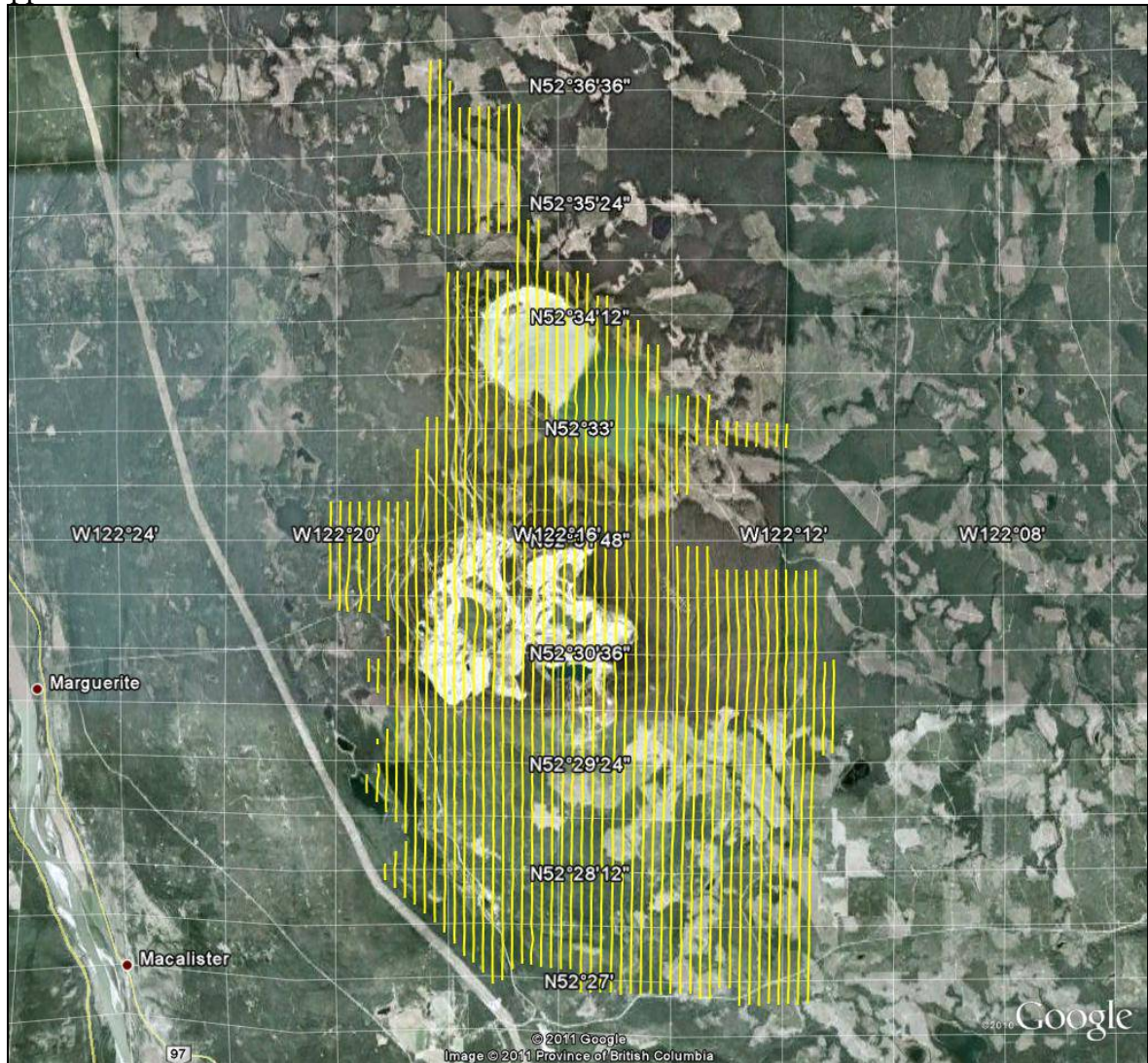


Figure 3 – Google Earth image of Survey Area

2. DATA ACQUISITION

2.1 Survey Area

The survey block (see Location map in Appendix A and Figure 2) and general flight specifications are as follows:

Table 1 - Survey Specifications

| Survey block | Traverse Line spacing (m) | Area (Km ²) | Line-km | Flight direction | Line numbers |
|----------------|---------------------------|-------------------------|--------------|-------------------|---------------|
| Gibraltar Mine | Traverse: 200 | 111 | 560.1 | N 0° E / N 180° E | L1000 – L1520 |
| | N/A | | | | |
| TOTAL | | 111 | 560.1 | | |

Survey block boundaries co-ordinates are provided in Appendix B.

2.2 Survey Operations

Survey operations were based out of Williams Lake, British Columbia on January 8th, 2011 until January 24th 2011. The following table shows the timing of the flying.

Table 2 - Survey schedule

| Date | Flight # | Block | Crew location | Comments |
|-------------|----------|----------------|-------------------|---------------------------------------|
| 8-Jan-2011 | | | Williams Lake, BC | Started system assembly |
| 9-Jan-2011 | | | Williams Lake, BC | System assembly |
| 10-Jan-2011 | | | Williams Lake, BC | System assembly completed |
| 11-Jan-2011 | | | Williams Lake, BC | System testing done |
| 12-Jan-2011 | | | Williams Lake, BC | ZTEM base to be repositioned |
| 13-Jan-2011 | | | Williams Lake, BC | No production due to weather |
| 14-Jan-2011 | | | Williams Lake, BC | No production due to weather |
| 15-Jan-2011 | | | Williams Lake, BC | No production due to weather |
| 16-Jan-2011 | 1 | Gibraltar Mine | Williams Lake, BC | Ground and air testing completed |
| 17-Jan-2011 | 2,3 | Gibraltar Mine | Williams Lake, BC | No production due to technical issues |
| 18-Jan-2011 | | | Williams Lake, BC | No production due to technical issues |
| 19-Jan-2011 | | | Williams Lake, BC | No production due to technical issues |
| 20-Jan-2011 | | | Williams Lake, BC | No production due to technical issues |
| 21-Jan-2011 | | | Williams Lake, BC | No production due to technical issues |
| 22-Jan-2011 | 4,5 | Gibraltar Mine | Williams Lake, BC | 440km flown |
| 23-Jan-2011 | 6,7 | Gibraltar Mine | Williams Lake, BC | 296km flown |
| 24-Jan-2011 | | | Williams Lake, BC | |

2.3 Flight Specifications

During the survey the helicopter was maintained at a mean height of 156 metres above the ground with a nominal survey speed of 80 km/hour for the survey block. This allowed for a nominal EM sensor terrain clearance of 82 metres and a magnetic sensor clearance of 99 metres.

The on-board operator was responsible for monitoring of the system integrity. He also maintained a detailed flight log during the survey, tracking the times of the flight as well as any unusual geophysical or topographic feature.

On return of the aircrew to the base camp the survey data was transferred from a compact flash card (PCMCIA) to the data processing computer. The data were then uploaded via ftp to the Geotech office in Aurora for daily quality assurance and quality control by trained personnel, operating remotely.

2.4 Aircraft and Equipment

2.4.1 Survey Aircraft

The survey was flown using a Geotech Aviation (Astar) 350 B3 helicopters, registration number C-GEOY. The helicopter was owned and operated by Geotech Aviation Ltd. Installation of the geophysical and ancillary equipment was carried out by Geotech Ltd.

2.4.2 Airborne Receiver

The airborne ZTEM receiver coil measures the vertical component (Z) of the EM field. The receiver coil is a Geotech Z-Axis Tipper (ZTEM) loop sensor which is isolated from most vibrations by a patented suspension system and is encased in a fibreglass shell. It is towed from the helicopter using a 90 metre long cable as shown in Figure 4. The cable is also used to transmit the measured EM signals back to the data acquisition system.

The coil has a 7.4 metre diameter with an orientation to the Vertical Dipole. The digitizing rate of the receiver is 2000 Hz. Attitudinal positioning of the receiver coil is enabled using 3 GPS antennas mounted on the coil. The output sampling rate is 0.4 seconds (see Section 2.4.7)

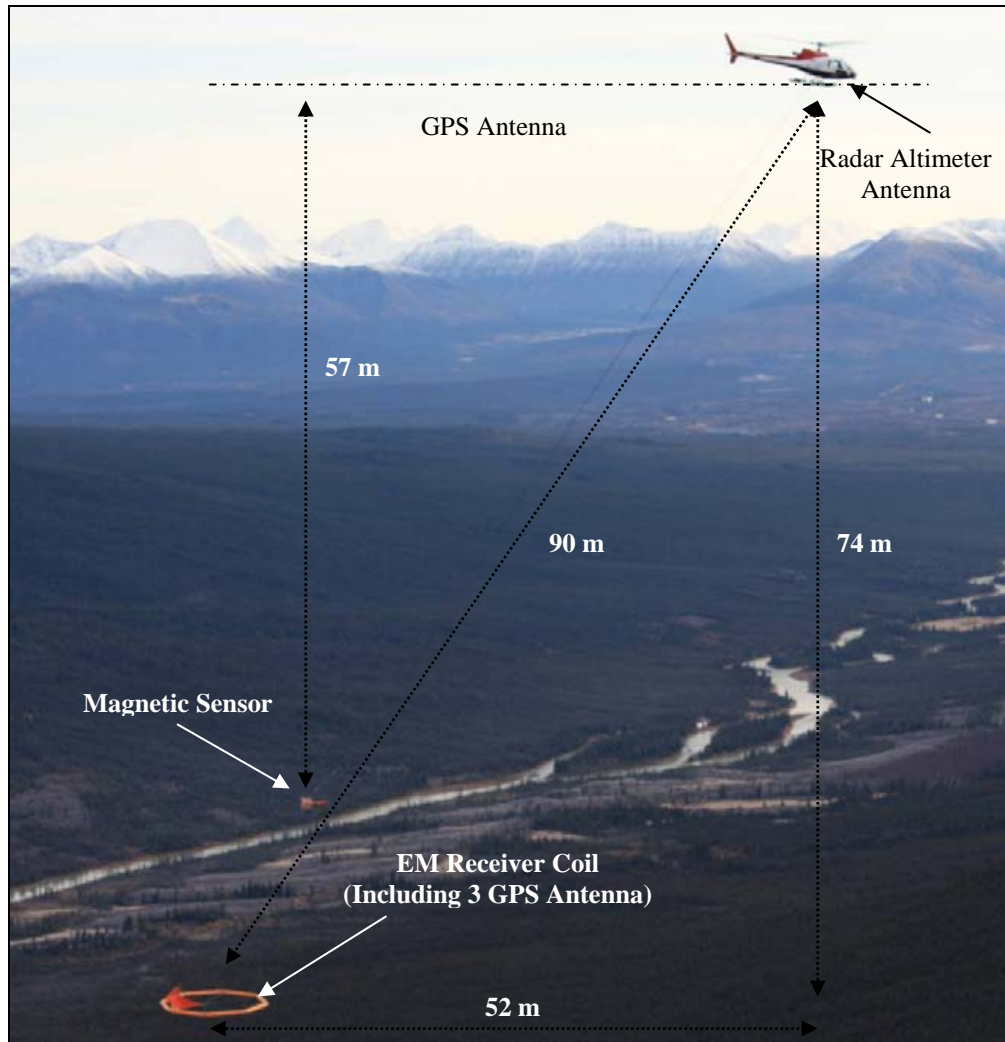


Figure 4 - ZTEM System Configuration

2.4.3 Base Station Receiver

The Geotech ZTEM base station consisted of two receiver coils which measure the orthogonal, horizontal X and Y components of the EM reference field. They are set up perpendicular to each other close to the survey area. The orientation of the base stations were measured using a compass.

The base station coils each have a diameter of 3.5 meters, with the coil orientations to the horizontal dipole, as shown in Figure 5.

The Block base station receiver coils were installed in a remote area near the survey block (52°26.34' N, 122°07.57.9' W). The coils were oriented perpendicular to each other: Coil A was oriented at an N 134° E direction, with coil B oriented at an N 224° E direction.



Figure 5 - ZTEM base station receiver coils.

2.4.4 Airborne magnetometer

The magnetic sensor utilized for the survey was a Geometrics split-beam optically pumped caesium vapour magnetic field sensor, mounted in a separate bird, and towed on a cable at a mean distance of 57 metres below the helicopter (Figure 4). The sensitivity of the magnetic sensor is 0.02 nanoTesla (nT) at a sampling interval of 0.1 seconds. The magnetometer will perform continuously in areas of high magnetic gradient with the ambient range of the sensor approximately 20k-100k nT. The Aerodynamic magnetometer noise is specified to be less than 0.5 nT. The magnetometer sends the measured magnetic field strength as nanoTesla to the data acquisition system via the RS-232 port.

2.4.5 Radar Altimeter

A Terra TRA 3000/TRI 40 radar altimeter was used to record terrain clearance. The antenna was mounted beneath the bubble of the helicopter cockpit.

2.4.6 GPS Navigation System

The navigation system used was a Geotech PC104 based navigation system utilizing a NovAtel CDGPS (Canada-Wide Differential Global Positioning System Correction Service) enabled Propak V3-RT20 GPS receiver. Geotech's Navigate software, using a full screen display with controls in front of the pilot, allows him to direct the flight.

5 NovAtel GPS antennas are utilized during the survey; one is mounted on the helicopter tail (Figure 4), one installed with the Receiver Base Station (Figure 5) and three are mounted on the airborne receiver (Figure 4). As many as 14 GPS and two CDGPS satellites may be monitored at any one time. The horizontal positional accuracy or circular error probability (CEP) is 1.8 m, with CDGPS active, it is 0.6 m. The co-ordinates of the block were set-up prior to the survey and the information was fed into the airborne navigation system.

2.4.7 Digital Acquisition System

The power supply and the data acquisition system are mounted on an equipment rack which is installed into the helicopter. Signal and power wires are run through the helicopter to connect on to the tow cable outside. The tow cable supports the ZTEM and magnetometer birds during flight via a safety shear pin connected to the helicopter hook. The major power and data cables have a quick disconnect safety feature as well. The installation was undertaken by the Geotech Ltd. crew and was certified before surveying.

A Geotech data acquisition system recorded the digital survey data on an internal compact flash card. Data is displayed on an LCD screen as traces to allow the operator to monitor the integrity of the system. The data type and sampling interval as provided in Table 3.

Table 3 - Acquisition and Processing Sampling Rates

| DATA TYPE | ACQUISITION SAMPLING | PROCESSING SAMPLING |
|-------------------|----------------------|---------------------|
| ZTEM Receiver | 0.0005 sec | 0.4 sec |
| Magnetometer | 0.1 sec | 0.4 sec |
| GPS Position | 0.2 sec | 0.4 sec |
| Radar Altimeter | 0.2 sec | 0.4 sec |
| ZTEM Base station | 0.0005 sec | -- |

2.4.8 Mag Base Station

A combined magnetometer/GPS base station was utilized on this project. A Geometrics Caesium split-beam vapour magnetometer was used as a magnetic sensor with a sensitivity of 0.001 nT. The base station was recording the magnetic field together with the GPS time at 1 Hz on a base station computer.

The base station magnetometer sensors for the Gibraltar Mines Property (52°11.15.35' N, 122°04.03.71' W) were installed on a hard bedrock area right next to the lake away from electric transmission lines and moving ferrous objects such as motor vehicles. The base station data were backed-up to the data processing computer at the end of each survey day.

3. PERSONNEL

The following Geotech Ltd. personnel were involved in the project.

Field:

| | |
|-------------------|----------------------|
| Project Manager: | Darren Tuck (Office) |
| Data QA/QC: | Nick Venter(Office) |
| Crew chief: | Brian Youngs |
| System Operators: | Brian Youngs |

The survey pilot and the mechanical engineer were employed directly by the helicopter operator –Geotech Aviation.

| | |
|----------------------|------------------|
| Pilot: | Geoffery Rawlins |
| Mechanical Engineer: | Yannick Provost |

Office:

| | |
|------------------------------|--------------|
| Preliminary Data Processing: | Nick Venter |
| Final Data Processing: | Alex Latrous |
| Final Data QC: | Ali Latrous |
| Reporting/Mapping: | Corrie Laver |

Data acquisition phase was carried out under the supervision of Andrei Bagrianski, P. Geo, Chief Operating Manager. Processing phase was carried out under the supervision of Harish Kumar, Assistant Manager of Data Processing. The overall contract management and customer relations were by Paolo Berardelli.

4. DATA PROCESSING AND PRESENTATION

Data compilation and processing were carried out by the application of Geosoft OASIS Montaj and programs proprietary to Geotech Ltd.

4.1 Flight Path

The flight path, recorded by the acquisition program as WGS 84 latitude/longitude, was converted into the WGS 84, UTM Zone 10 North coordinate system in Oasis Montaj.

The flight path was drawn using linear interpolation between x, y positions from the navigation system. Positions are updated every second and expressed as UTM easting's (x) and UTM northing's (y).

4.2 In-field Processing and Quality Control

In-Field data processing and quality control are done on a flight by flight basis by a qualified data processor (see Section 3.0). Processing steps and check up procedures are designed to assure the best possible final quality of ZTEM survey data. A general overview of those steps is presented in the following paragraphs.

The In-Field quality control can be separated into several phases:

- a. GPS Processing Phase: GPS Data are first examined and evaluated during the GrafMov processing.
- b. Raw data, ZTEM viewer phase:

Data can be viewed, examined for consistency, individual channel spectra examined and overall noise estimated in the viewer provided by the ZTEM proprietary software, on the raw flight data and raw base station data separately, on the merged data, and finally on the data that have undergone ZTEM processing.
- c. Field Geosoft phase:

Magnetic data, Radar altimeter data, GPS positioning data are re-examined and processed in this phase. Prior to splitting the lines EM data are examined flight by flight and the effectiveness of applying the attitude correction evaluated. After splitting the lines, a set of grids are generate for each parameter and their consistency evaluated. Data profiles are also re-evaluated on a line to line basis. A power line monitor channel is available in order to identify power line noise.

4.3 GPS Processing

Three GPS sensor (mounted on the airborne receiving loop) measurements were differentially corrected using the Waypoint GrafMovTM software in order to yield attitude corrections to recorded EM data.

4.4 ZTEM Electromagnetic Data

The ZTEM data were processed using proprietary software. Processing steps consist of the following preliminary and final processing steps:

4.4.1 Preliminary Processing

- a. Airborne EM, Mag, radar altimeter and GPS data are first merged with EM base station data into one file.
- b. Merged data are viewed and examined for consistency in an incorporated viewer
- c. In the next, processing phase, the following entities are taken into account:
 - the Base station coils orientation with respect to the Magnetic North,
 - the Local declination of the magnetic field,
 - Suggested direction of the X coordinate (North or line direction),
 - Sensitivity coefficient that compensates for the difference in geometry between the base station and airborne coils.
 - Rejection filters for the 60 Hz and helicopter generated frequencies.
- d. Six frequencies (30, 45, 90, 180 & 360Hz) are extracted from the airborne EM time-series coil response using windows of 0.4 seconds and the base station coils using windows of 1.0 seconds.
- e. The real (In-Phase) and imaginary (Quadrature) parts of the tipper transfer functions are derived from the In-line (X or Tzx) and Cross-line (Y or Tzy) components.
- f. Such processed EM data are then merged with the GPS data, magnetic base station data and exported into a Geosoft xyz file.

4.4.2 Geosoft Processing

Next stage of the preliminary data processing is done in a Geosoft™ environment, using the following steps:

- a. Import the output xyz file from the AFMAG processing, as well as the base Mag data into one database.
- b. Split lines according to the recorded line channel,
- c. GPS processing, flight path recovery (correcting, filtering, calculating Bird GPS coordinates, line splitting)
- d. Radar altimeter processing, yielding the altitude values in metres.
- e. Magnetic spike removal, filtering (applied to both airborne and base station data). Calculation of a base station corrected mag.
- f. Apply preliminary attitude corrections to EM data (In phase and Quadrature), filter and make preliminary grids and profiles of all channels.

4.4.3 Final Processing

Final data processing and quality control were undertaken by Geotech Ltd headquarters in Aurora, Ontario by qualified senior data processing personnel.

A quality control step consisted of re-examining all data in order to validate the preliminary data processing and to allow for final adjustments to the data.

Attitude corrections were re-evaluated, and re-applied, on component by component, flight by flight, and frequency by frequency bases. Any remaining line to line system noise was removed by applying a mild additional levelling correction.

4.4.4 ZTEM Profile Sign Convention

Tzx and Tzy tipper components do not exhibit maxima or minima above conductors, resistors or at contacts; in fact they produce cross-over type anomalies (Ward, 1959; Vozoff, 1972; Labson, 1985). The crossover polarity sign convention for ZTEM is according to the right hand Cartesian rule (Z positive –up) that is commonly used for multi-component transient electromagnetic methods.

For the North to South lines at the Block the sign convention for the Tzx in-line component crossover is positive-negative pointing South to North for tabular conductors perpendicular to the profile (Figure 6). The corresponding Tzy component in-phase cross-over polarity is positive-negative pointing East to West (90 degrees counter clockwise to Tzx) according to the right hand Cartesian rule.

Conversely, tabular resistive bodies produce In-Phase cross-over's that are opposite in sign to conductors. A brief discussion of ZTEM and AFMAG, along with selected forward model responses is presented in Appendix D.

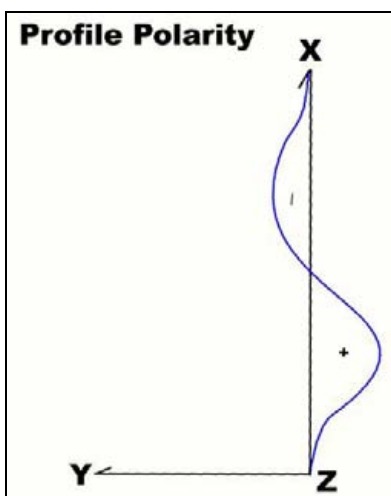


Figure 6 - ZTEM Crossover Polarity Convention for Tzx and Tzy

4.4.5 ZTEM Quadrature Sign Dependence

One important note regarding the sign of the ZTEM Quadrature, relative to the In-Phase component, particularly with regards to computer modeling and inversion.

The sign of the magnetotelluric Quadrature relative to the In-Phase tipper transfer function component pertains to the Fourier transformation of the time series to give frequency domain spectra. There are two widely used conventions for time dependence in the transformations, $\exp(+i\omega t)$ and $\exp(-i\omega t)$. That which is implemented largely is a matter of personal preference and precedent. The importance of the In-Phase and Quadrature sign convention is not critical, provided that it is known and documented.

In ZTEM, the data processing code used for the Fourier transformation the time-series data to frequency domain spectra adopts a $\exp(-i\omega t)$ time dependence (J. Dodds, Geo Equipment Manufacturing, pers. comm., Nov-2009). Whereas in the forward modeling and inversion program Zvert2d, the sign of the Quadrature relative to the In-Phase transfer function assumes an $\exp(+i\omega t)$ dependence¹.

The reasons for adopting $e^{-i\omega t}$ used in ZTEM are several: a) In-phase and Quadrature profile and contour plan maps can be readily compared, since they are usually in the same-sign and quadrant (i.e. Figure 7); b) Phase-rotation and Total Divergence (DT) parameters need not be changed when comparing In-Phase versus Quadrature data.

As a result, for users interested in computer modeling and inversion of ZTEM data, the sign of the Quadrature will need to be reversed, relative to the In-Phase component, in order to provide a proper result (Figure 7). Indeed this reverse Quadrature polarity convention is assumed in all forward modeling and inversion of ZTEM data, as described in Figures 5-7 in Appendix D.

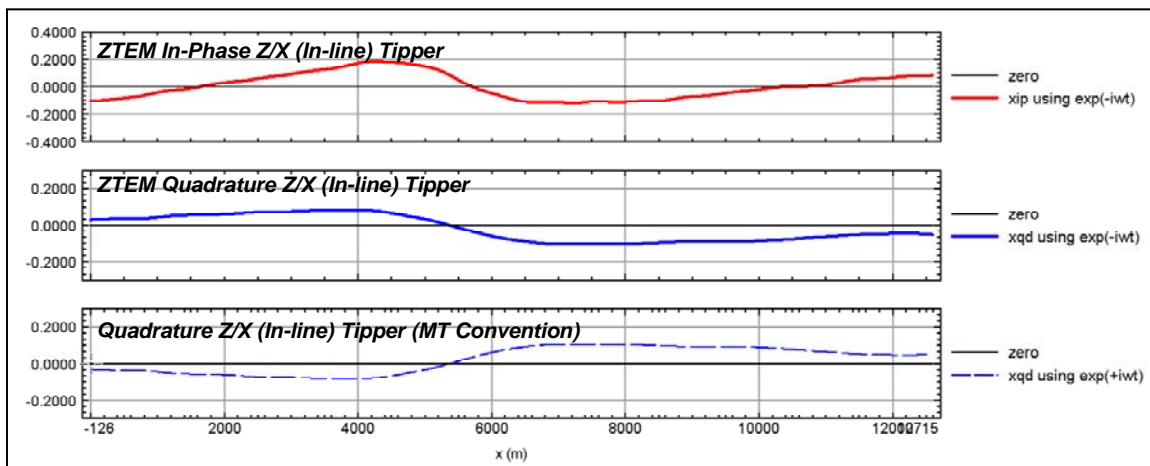


Figure 7 - Illustration of ZTEM In-Phase & Quadrature Tipper transfer function polarity convention ($e^{-i\omega t}$) relative to equivalent MT Tipper Quadrature polarity convention ($e^{+i\omega t}$) for a graphitic conductor in Athabasca Basin, SK.

¹ Phillip E. Wannamaker (2009): Two-dimensional Inversion of ZTEM data: Synthetic Model Study and Test Profile Images, Internal Geotech technical report by Emblem Exploration Services Inc., January 22, 2009, 32 pp.

4.4.6 Total Divergence and Phase Rotation Processing

In a final processing step DT (Total Divergence) and PR (Phase Rotation) processing are applied to the multi-frequency In-phase and Quadrature ZTEM data. This is due to the crossover nature of the Tipper Responses; these additional processing steps are applied to convert them into local maxima for easier interpretation.

To present the data from both tipper components into one image, the Total Divergence parameter, termed the DT is calculated from the horizontal derivatives of the Tzx and Tzy tippers (Lo and Zang, 2008). It is analogous to the “Peaker” parameter in VLF (Pedersen, 1998).

$$\textit{Total Divergence DT:} \quad DT = DIV (Tzx, Tzy) \\ = d(Tzx)/dx + d(Tzy)/dy$$

This DT parameter was introduced by Petr Kuzmin (Milicevic, 2007, p. 13) and is derived for each of the In Phase and Quadrature components at individual frequencies. These in turn allow for minima over conductors and maxima over resistive zones. DT grids for each of the extracted frequencies were generated accordingly, using a reverse colour scheme with warm colours over conductors and cool colours over resistors.

The DT gives a clearer image of conductor’s location and shape but, as a derivative, it does not preserve some of the long wavelength information and is also sensitive to noise.

As an alternative, a 90 degree Phase Rotation (PR) technique is also applied to the grids of each individual component (Tzx and Tzy). It transforms bipolar (cross over) anomalies into single pole anomalies with a maximum over conductors, while preserving long wavelength information (Lo et al., 2009). The two orthogonal grids are then usually added to obtain a Total Phase Rotated grid for the In-Phase and Quadrature.

$$\textit{Total Phase-Rotation:} \quad = PR (Tzx) + PR (Tzy)$$

A presentation of the ZTEM test survey results over unconformity uranium deposits that illustrates DT and TPR examples, as documented by Lo et al. (2009) is provided in Appendix E.

4.5 Magnetic Data

The processing of the total magnetic field intensity (TMI) data involved the correction for diurnal variations by using the digitally recorded ground base station magnetic values. The base station magnetometer data was edited and merged into the Geosoft GDB database on a daily basis. The aeromagnetic data was corrected for diurnal variations by subtracting the observed magnetic base station deviations.

Due to the absence of tie-lines, further tie-line or micro levelling were not applied to the magnetic data.

The corrected magnetic data was interpolated between survey lines using a random point gridding method to yield x-y grid values for a standard grid cell size of 50 metres. The Minimum Curvature algorithm was used to interpolate values onto a rectangular regular spaced grid.

5. DELIVERABLES

5.1 Survey Report

The survey report describes the data acquisition, processing, and final presentation of the survey results. The survey report is provided in two paper copies and digitally in PDF format.

5.2 Maps

Final maps were produced at scale of 1:20,000. The coordinate/projection system used was WGS84, UTM Zone 10 North. All maps show the flight path trace and topographic data; latitude and longitude are also noted on maps.

The preliminary and final results of the survey are presented as profile plans for the EM data that were generated for individual real (In-Phase) and imaginary parts (Quadrature) of the Tzx and Tzy components. Colour contour maps of the corresponding DT (Total Divergence) or TPR (Total Phase Rotated) grids for three of the five frequencies, (30, 45, 90, 180 and 360Hz), as well as for corresponding Phase Rotated Grids for individual components.

3D views have been constructed by plotting the either DT or TPR grids at their respective penetration depths using a 1000 ohm-m half space, using the Bostick skin depth rule (Bostick, 1977) see Appendix D.

Final maps were chosen, in consultation with the client, to represent all collected data, are listed in Section 5.3.

Sample maps of the related 3D view, Magnetic and Total Divergence are included in this report and presented in Appendix C.

5.3 Digital Data

- Two copies of the data and maps on a DVD were prepared to accompany the report. Each DVD contains a digital file of the line data in GDB Geosoft Montaj.
- DVD structure.
 - There are two (2) main directories;
 - Data:** contains databases, Geosoft grids, Geosoft & PDF maps, as described below.
 - Report:** contains a copy of the report and appendices in PDF format.

Databases in Geosoft GDB format, containing the channels listed in Table 4.

Table 4 - Geosoft GDB Data Format

| Column | Description |
|---------------|--|
| X: | UTM Easting WGS84 Zone 10N, (Centre of the ZTEM loop) (meters) |
| Y: | UTM Northing WGS84 Zone 10N , (Centre of the ZTEM loop) (meters) |
| Longitude: | Longitude – WGS84 (Centre of the ZTEM loop) (Decimal degree) |
| Latitude | Latitude – WGS84 (Centre of the ZTEM loop) (Decimal degree) |
| Z: | Elevation- WGS84 (Centre of the ZTEM loop) (metres) |
| Radar: | Helicopter terrain clearance from radar altimeter (metres - AGL) |
| Radar_B: | Calculated ZTEM Bird terrain clearance (metres) |
| DEM | Digital Elevation Model (meters) |
| Gtime | GPS Time (seconds) |
| basemag | Base station mag |
| Mag1 | Measured Total Magnetic Intensity, raw (de-spiked) |
| Mag2 | Measured Total Magnetic Intensity, diurnal corrected |
| Mag3: | Levelled Total Magnetic field data |
| xIp_030Hz: | Tzx In-Phase 30 Hz final corrected |
| xIp_045Hz: | Tzx In-Phase 45 Hz final corrected |
| xIp_090Hz: | Tzx In-Phase 90 Hz final corrected |
| xIp_180Hz: | Tzx In-Phase 180 Hz final corrected |
| xIp_360Hz: | Tzx In-Phase 360 Hz final corrected |
| xQd_030Hz: | Tzx Quadrature 30 Hz final corrected |
| xQd_045Hz: | Tzx Quadrature 45 Hz final corrected |
| xQd_090Hz: | Tzx Quadrature 90 Hz final corrected |
| xQd_180Hz: | Tzx Quadrature 180 Hz final corrected |
| xQd_360Hz: | Tzx Quadrature 360 Hz final corrected |
| yIp_030Hz: | Tzy In-Phase 30 Hz final corrected |
| yIp_045Hz: | Tzy In-Phase 45 Hz final corrected |
| yIp_090Hz: | Tzy In-Phase 90 Hz final corrected |
| yIp_180Hz: | Tzy In-Phase 180 Hz final corrected |
| yIp_360Hz: | Tzy In-Phase 360 Hz final corrected |
| yQd_030Hz: | Tzy Quadrature 30 Hz final corrected |
| yQd_045Hz: | Tzy Quadrature 45 Hz final corrected |
| yQd_090Hz: | Tzy Quadrature 90 Hz final corrected |
| yQd_180Hz: | Tzy Quadrature 180 Hz final corrected |
| yQd_360Hz: | Tzy Quadrature 360 Hz final corrected |
| PLM: | Power Line Monitor (60Hz) |

- Grids in Geosoft GRD format, as follows:

| | |
|---------------|---|
| MAG: | Total Magnetic Intensity |
| DEM: | Digital Elevation Model |
| XIP_30Hz_PR: | Tzx In-Phase Component Phase Rotated grid at 30 Hz |
| XIP_45Hz_PR: | Tzx In-Phase Component Phase Rotated grid at 45 Hz |
| XIP_90Hz_PR: | Tzx In-Phase Component Phase Rotated grid at 90 Hz |
| XIP_180Hz_PR: | Tzx In-Phase Component Phase Rotated grid at 180 Hz |
| XIP_360Hz_PR: | Tzx In-Phase Component Phase Rotated grid at 360 Hz |
| XQd_30Hz_PR: | Tzx Quadrature component Phase Rotated grid at 30 Hz |
| XQd_45Hz_PR: | Tzx Quadrature component Phase Rotated grid at 45 Hz |
| XQd_90Hz_PR: | Tzx Quadrature component Phase Rotated grid at 90 Hz |
| XQd_180Hz_PR: | Tzx Quadrature component Phase Rotated grid at 180 Hz |
| XQd_360Hz_PR: | Tzx Quadrature component Phase Rotated grid at 360 Hz |
| YIP_30Hz_PR: | Tzy In-Phase Component Phase Rotated grid at 30 Hz |
| YIP_45Hz_PR: | Tzy In-Phase Component Phase Rotated grid at 45 Hz |
| YIP_90Hz_PR: | Tzy In-Phase Component Phase Rotated grid at 90 Hz |
| YIP_180Hz_PR: | Tzy In-Phase Component Phase Rotated grid at 180 Hz |
| YIP_360Hz_PR: | Tzy In-Phase Component Phase Rotated grid at 360 Hz |
| YQd_30Hz_PR: | Tzy Quadrature component Phase Rotated grid at 30 Hz |
| YQd_45Hz_PR: | Tzy Quadrature component Phase Rotated grid at 45 Hz |
| YQd_90Hz_PR: | Tzy Quadrature component Phase Rotated grid at 90 Hz |
| YQd_180Hz_PR: | Tzy Quadrature component Phase Rotated grid at 180 Hz |
| YQd_360Hz_PR: | Tzy Quadrature component Phase Rotated grid at 360 Hz |
| IP_30Hz_DT: | Total Divergence grid from In-phase components at 30 Hz |
| IP_45Hz_DT: | Total Divergence grid from In-phase components at 45 Hz |
| IP_90Hz_DT: | Total Divergence grid from In-phase components at 90 Hz |
| IP_180Hz_DT: | Total Divergence grid from In-phase components at 180 Hz |
| IP_360Hz_DT: | Total Divergence grid from In-phase components at 360 Hz |
| QD_30Hz_DT: | Total Divergence grid from Quadrature components at 30 Hz |
| QD_45Hz_DT: | Total Divergence grid from Quadrature components at 45 Hz |
| QD_90Hz_DT: | Total Divergence grid from Quadrature components at 90 Hz |
| QD_180Hz_DT: | Total Divergence grid from Quadrature components at 180 Hz |
| QD_360Hz_DT: | Total Divergence grid from Quadrature components at 360 Hz |
| IP_30Hz_TPR: | Total Phase Rotated grid from In-phase components at 30 Hz |
| IP_45Hz_TPR: | Total Phase Rotated grid from In-phase components at 45 Hz |
| IP_90Hz_TPR: | Total Phase Rotated grid from In-phase components at 90 Hz |
| IP_180Hz_TPR: | Total Phase Rotated grid from In-phase components at 180 Hz |
| IP_360Hz_TPR: | Total Phase Rotated grid from In-phase components at 360 Hz |
| QD_30Hz_TPR: | Total Phase Rotated grid from Quadrature components at 30 Hz |
| QD_45Hz_TPR: | Total Phase Rotated grid from Quadrature components at 45 Hz |
| QD_90Hz_TPR: | Total Phase Rotated grid from Quadrature components at 90 Hz |
| QD_180Hz_TPR: | Total Phase Rotated grid from Quadrature components at 180 Hz |
| QD_360Hz_TPR: | Total Phase Rotated grid from Quadrature components at 360 Hz |

A Geosoft .GRD file has a .GI metadata file associated with it, containing grid projection information. A grid cell size of 50 metres was used.

- Maps at 1:20,000 scale in Geosoft MAP format, as follows:

10105_20K_TMI Clipped: Total Magnetic Intensity (TMI)

10105_20K_3D_IP_TPR Clipped: View of In-Phase Total Phase Rotated Grids versus Bostick Skin Depth

10105_20K_30Hz_XIP_PR_Clippped:30Hz Tzx Component In-Phase Phase Rotated

10105_20K_90Hz_XIP_PR_Clippped:90Hz Tzx Component In-Phase Phase Rotated

10105_20K_360Hz_XIP_PR_Clippped:360Hz Tzx Component In-Phase Phase Rotated

10105_20K_30Hz_IP_TPR_Clippped: 30Hz In-Phase Total Phase Rotated Grid

10105_20K_90Hz_IP_TPR_Clippped: 90Hz In-Phase Total Phase Rotated Grid

10105_20K_360Hz_IP_TPR_Clippped: 360Hz In-Phase Total Phase Rotated Grid

10105_20K_30Hz_QD_DT_Clippped: 30Hz Quadrature Total Divergence Grid

10105_20K_90Hz_QD_DT_Clippped: 90Hz Quadrature Total Divergence Grid

10105_20K_360Hz_QD_DT_Clippped: 360Hz Quadrature Total Divergence Grid

10105_20k_90Hz_IP_DT_Clippped: 90 Hz In-Phase Total Divergence Grid

10105_20k_180_IP_DT_Clippped: 90 Hz In-Phase Total Divergence Grid

10105_20K_XIP_profiles_XIP_PR_Clippped: Tzx (In-line) In-Phase Profiles over 90Hz Phase Rotated In-Phase Grid

10105_20K_XQD_profiles_XQD_PR_Clippped:Tzx (In-line) Quadrature Profiles over a 90Hz Phase Rotated Quadrature Grid.

10105_20K_YIP_profiles_YIP_PR_Clippped:Tzy(Cross-line) In-Phase Profiles over 90Hz Phase Rotated In-Phase Grid

10105_20K_YQD_profiles_YQD_PR_Clippped:Tzy (Cross-line) Quadrature Profiles over a 90Hz Phase Rotated Quadrature Grid.

- Maps are also presented in PDF format.

1:50,000 topographic vectors were taken from the NRCAN Geogratis database at; <http://geogratis.gc.ca/geogratis/en/index.html>.

Mining Claims are derived from the British Columbia Government Land and Resources Data Warehouse: <http://aardvark.gov.bc.ca>

- A Google Earth file “10105_Gibraltar_Clippped.kml” is included, showing the flight path of each block. Free versions of Google Earth software from: <http://earth.google.com/download-earth.html>.

6. CONCLUSIONS AND RECOMMENDATIONS

6.1 Conclusions

A helicopter-borne ZTEM and aeromagnetic geophysical survey has been completed over the Gibraltar Mine Property clipped to the mineral property boundary located near McLeese Lake, British Columbia.

The total area coverage is 111 km². Total survey line coverage clipped to the mineral claims boundary is 560.1 line kilometres. The principal sensors included a Z-Axis Tipper electromagnetic (ZTEM) system and a caesium magnetometer. Results have been presented as stacked profiles and contour colour images at a scale of 1:20,000.

There is no summary interpretation included in this report.

6.2 Recommendations

Based on the geophysical results obtained, a number of interesting conductive structures were identified across the property. The magnetic results also contain worthwhile information in support of exploration targets of interest. We therefore recommend a more detailed interpretation of the available geophysical data, including VTEM, in conjunction with the geology, prior to ground follow up and drill testing.

Respectfully submitted⁶,

Ali Latrous, MSc
Geotech Ltd.

Jean Legault, P. Geo, P. Eng
Geotech Ltd.

Harish Kumar, P. Geo
Geotech Ltd.

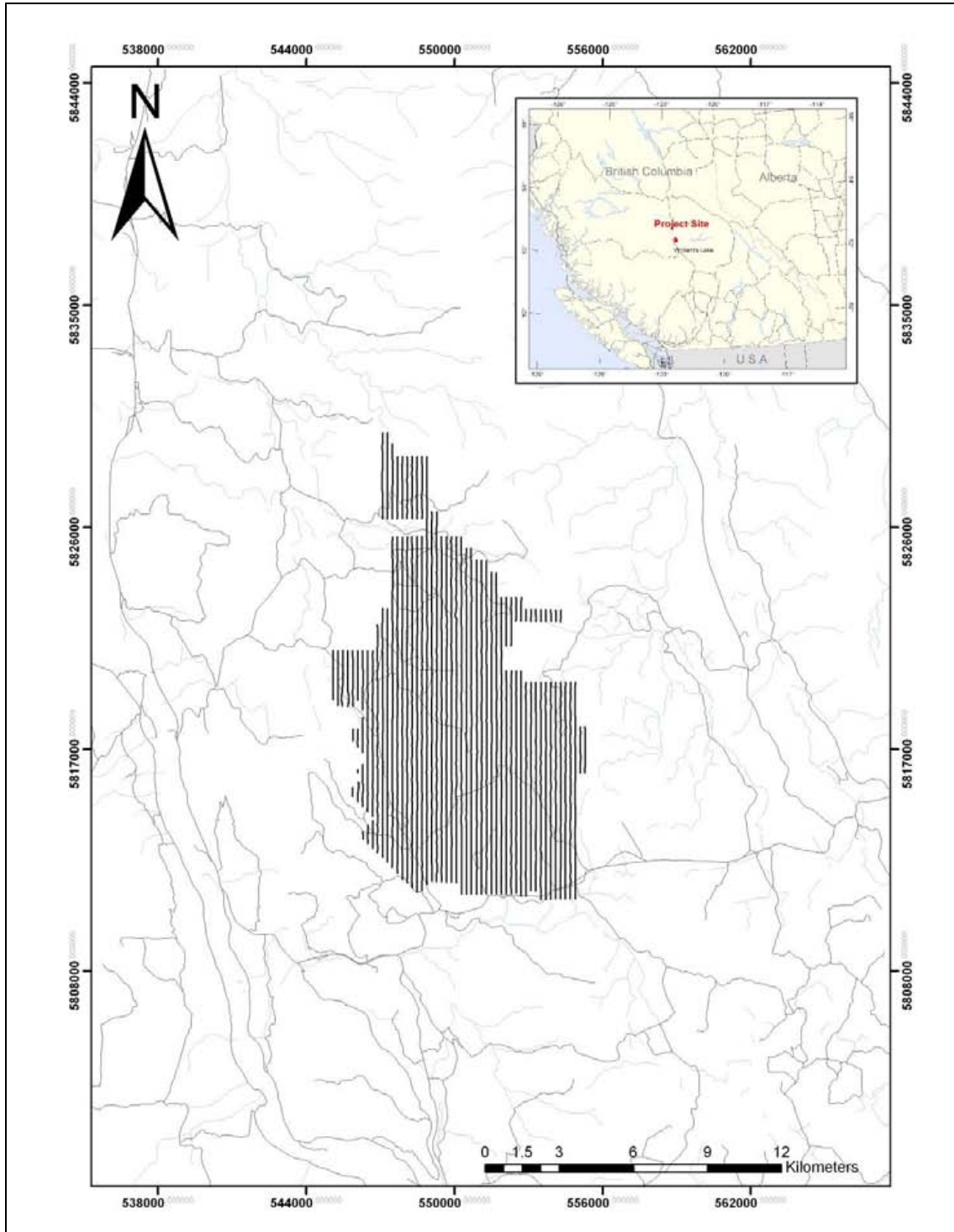
March 2011

⁶ Final data processing of the EM and magnetic data were carried out by Ali Latrous from the office of Geotech Ltd. in Aurora, Ontario, under the supervision of Harish Kumar, Assistant Manager of Data Processing, also under the supervision of Jean Legault, P. Geo, P. Eng, Chief Geophysicist (Interpretation)

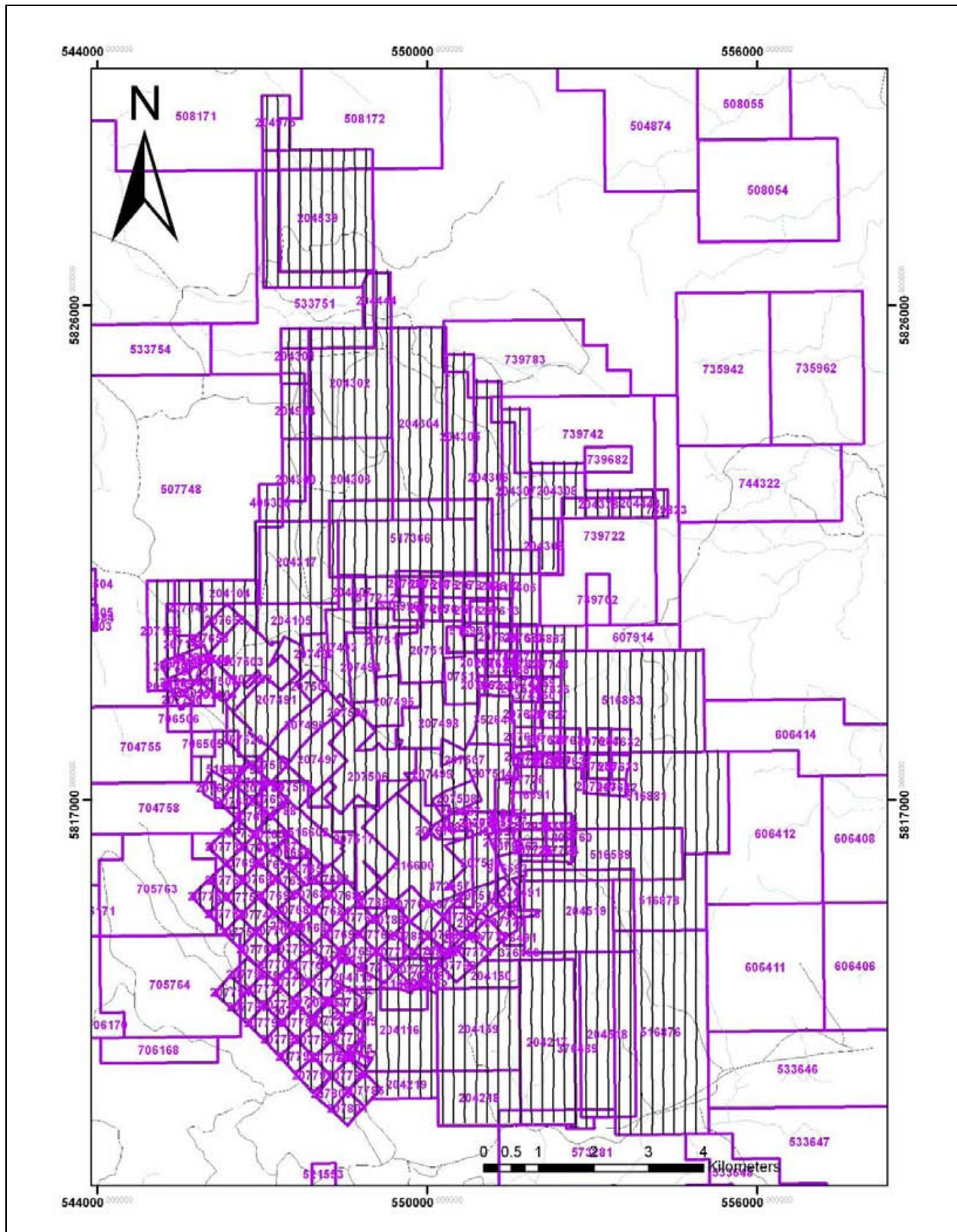
7. REFERENCES AND SELECTED BIBLIOGRAPHY

- Anav, A., Cantarano, S., Cerruli-Irelli, P., and Pallotino, G.V.(1976). A correlation method for measurement of variable magnetic fields: *Inst. Elect. and Electron. Eng. Trans., Geosc. Elect.* GE14, 106-114.
- Bostick, F.X. (1977). A Simple almost exact method of MT analysis, Proceedings of the University of Utah Workshop on Electrical Methods in Geothermal Exploration, 175-188.
- De Lugao, P.P.,and Wannamaker, P.E.(1996). Calculating the two-dimensional magnetotelluric Jacodian in finite elements using reciprocity: *Geophys. J. Int.*, **127**, 806-810
- Karous, M.R., and S. E. Hjelt (1983). Linear filtering of VLF dip-angle measurements: *Geophysical Prospecting*, **31**, 782-794.
- Kuzmin, P., Lo, B. and Morrison, E. (2005). Final Report on Modeling, interpretation methods and field trials of an existing prototype AFMAG system, Miscellaneous Data Release 167, Ontario Geological Survey, 2005.
- Labson, V. F., Becker A., Morrison, H. F., and Conti, U. (1985). Geophysical exploration with audiofrequency natural magnetic fields. *Geophysics*, **50**, 656-664.
- Legault, J.M., Kumar, H., Milicevic, B., and Hulbert, L. (2009), ZTEM airborne tipper AFMAG test survey over a magmatic copper-nickel target at Axis Lake in northern Saskatchewan, SEG Expanded Abstracts, **28**, 1272-1276
- Legault, J.M., Kumar, H., Milicevic, B., and Wannamaker, P.,(2009), ZTEM tipper AFMAG and 2D inversion results over an unconformity uranium target in northern Saskatchewan, SEG Expanded Abstracts, **28**, 1277-1281.
- Lo, B., Legault, J.M., Kuzmin, P. and Combrick, M. (2009). ZTEM (Airborne AFMAG) tests over unconformity uranium deposits, Extended abstract submitted to 20th ASEG International Conference and Exhibition, Adelaide, AU, 4pp.
- Lo, B., and Zang, M., (2008), Numerical modeling of Z-TEM (airborne AFMAG) responses to guide exploration strategies, SEG Expanded Abstracts, **27**, 1098-1101.
- Milicevic, B. (2007). Report on a helicopter borne Z-axis, Tipper electromagnetic (ZTEM) and magnetic survey at Safford, Giant Hills, Baldy Mountains and Sierrita South Areas, Arizona, USA., Geotech internal survey report (job A226), 33pp.
- Pedersen, L.B., Qian, W., Dynesius, L. and Zhang, P. (1994). An airborne sensor VLF system. From concept to realization. *Geophysical Prospecting*, **42**, i.8, 863-883
- Peterson, L.B. (1998). Tensor VLF measurements: first experiences, *Exploration Geophysics*, **29**, 52-57.
- Strangway, D. W., Swift Jr., C. M., and Holmer, R. C. (1973). The Application of Audio-Frequency Magnetotellurics (AMT) to Mineral Exploration. *Geophysics*, **38**, 1159-1175.
- Tarantola, A.,(1987) Inverse problem theory: Elsevier, New York, 613 pp.
- Vozoff, K.(1972). The magnetotelluric method in the exploration of sedimentary basins. *Geophysics*, **37**, 98-141.
- Vozoff, K. (1991). The magnetotelluric method. In: Electromagnetic Methods in Applied Geophysics - Volume 2 Applications, edited by Nabighian, M.N., Society of Exploration Geophysicists, Tulsa., 641-711.
- Ward, S. H. (1959). AFMAG - Airborne and Ground. *Geophysics*, **24**, 761-787.
- Ward, S. H, O'Brien, D.P., Parry, J.R. and McKnight, B.K. (1968). AFMAG Interpretation. *Geophysics*, **33**, 621-644.
- Wannamaker, P.E., Stodt, J.A., and Rijo, L., (1987). A stable finite element solution for two-dimensional magnetotelluric modeling: *Geophy. J. Roy. Astr. Soc.*,**88**, 277-296.
- Zhang, P. and King, A. (1998). Using magnetotellurics for mineral exploration, Extended Abstracts from 1998 Meeting of Society of Exploration Geophysics

APPENDIX A
SURVEY BLOCK LOCATION MAP



Survey Overview Location Map



Mining Claims for the Gibraltar Mine (Clipped)

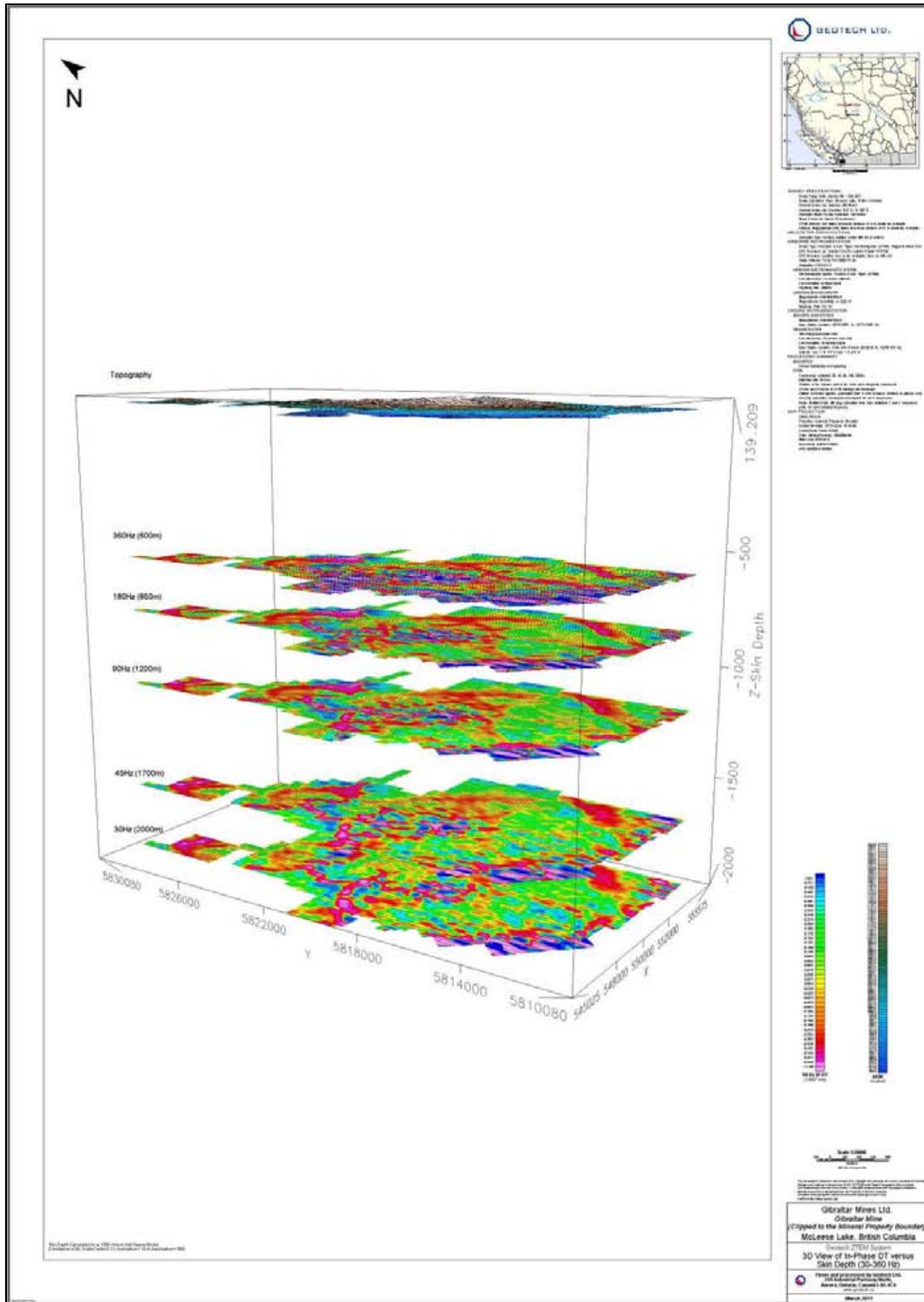
APPENDIX B

SURVEY BLOCK COORDINATES

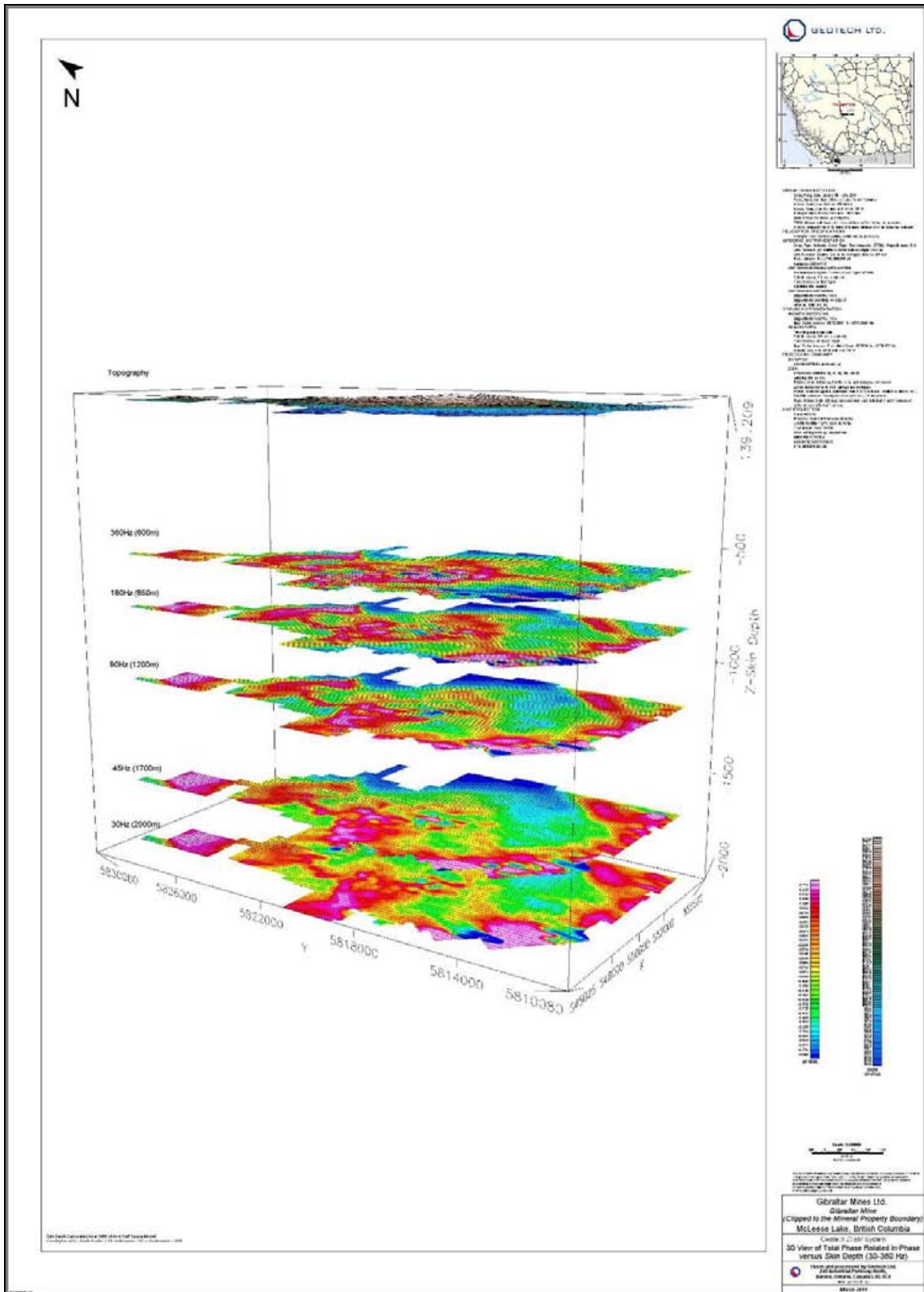
(WGS 84, UTM Zone 10 North)

| X | Y |
|----------|---------|
| 546996.6 | 5829815 |
| 547506.3 | 5829820 |
| 547506.3 | 5828820 |
| 549029.2 | 5828835 |
| 549029.2 | 5826588 |
| 549341.5 | 5826592 |
| 549341.5 | 5825591 |
| 550346.5 | 5825602 |
| 550346.5 | 5825102 |
| 550851.3 | 5825107 |
| 550851.3 | 5824606 |
| 551356.1 | 5824611 |
| 551356.1 | 5824111 |
| 551866.6 | 5824117 |
| 551866.6 | 5823116 |
| 552871.8 | 5823127 |
| 552871.8 | 5822627 |
| 554377.1 | 5822643 |
| 554377.1 | 5820927 |
| 555494.9 | 5820927 |
| 555494.9 | 5810361 |
| 548023.5 | 5810361 |
| 548023.5 | 5811079 |
| 544904.9 | 5813989 |
| 544942.6 | 5825004 |
| 546996.6 | 5825004 |

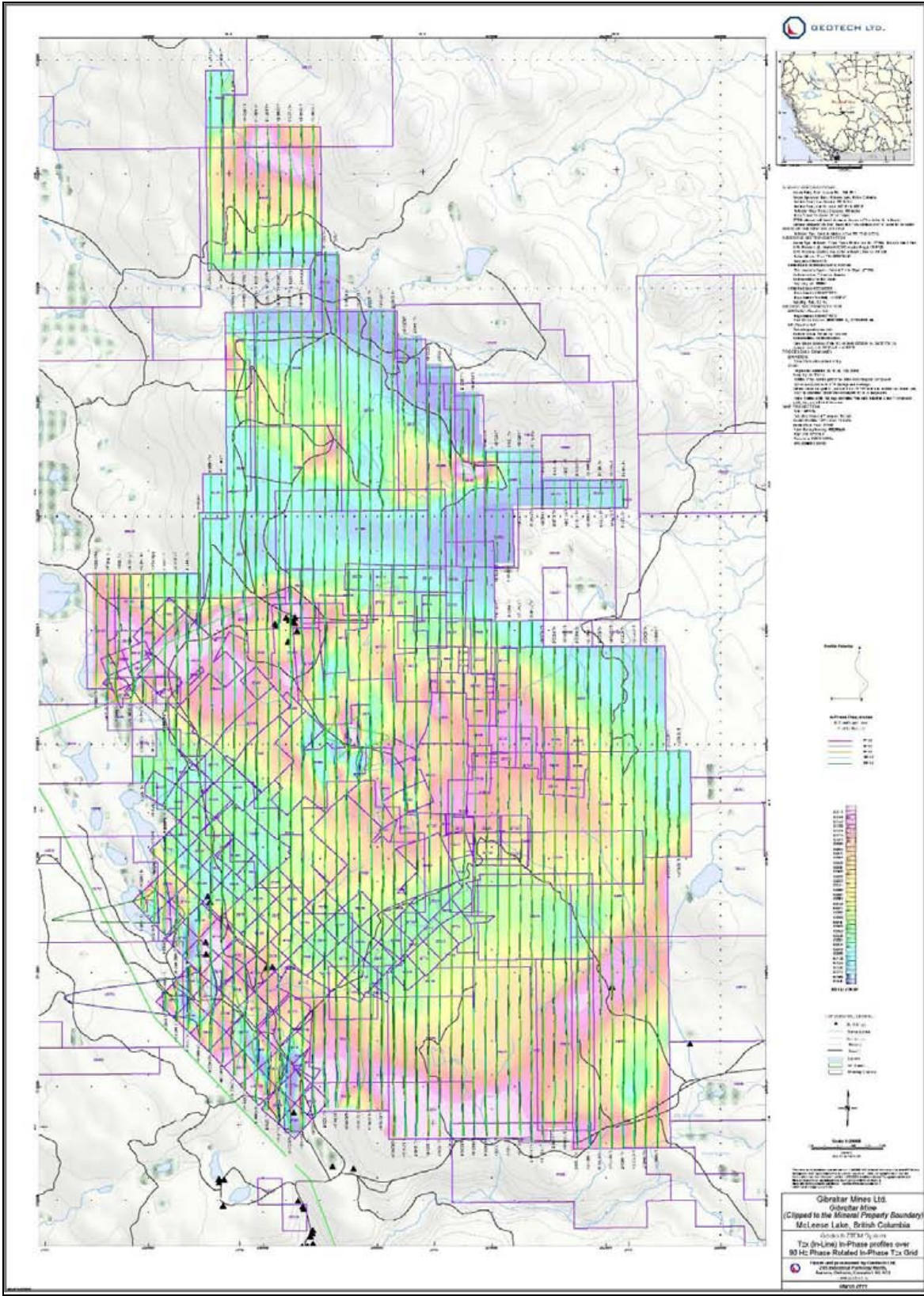
APPENDIX C GEOPHYSICAL MAPS¹



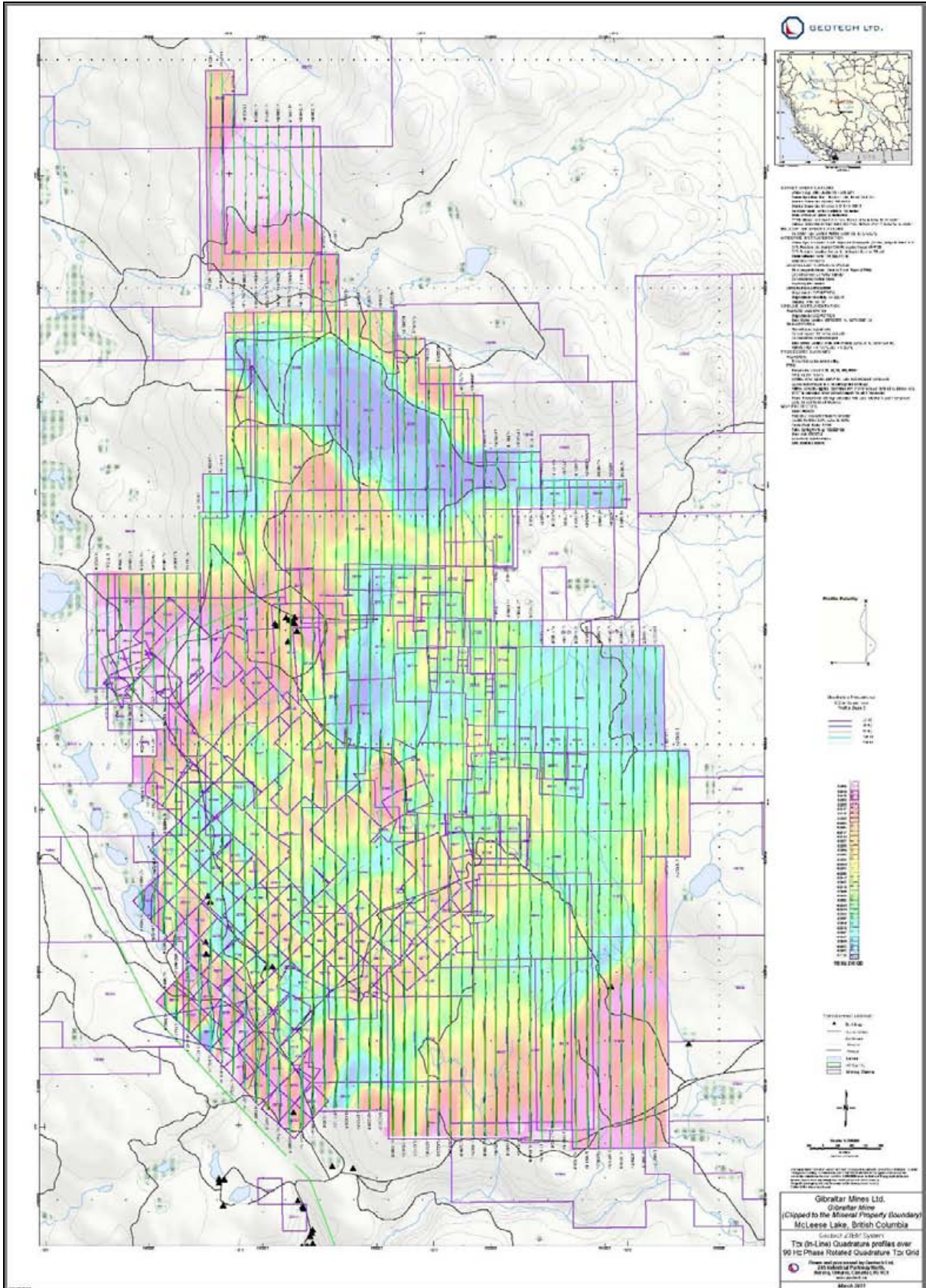
¹ Full size geophysical maps are also available in PDF format on the final DVD



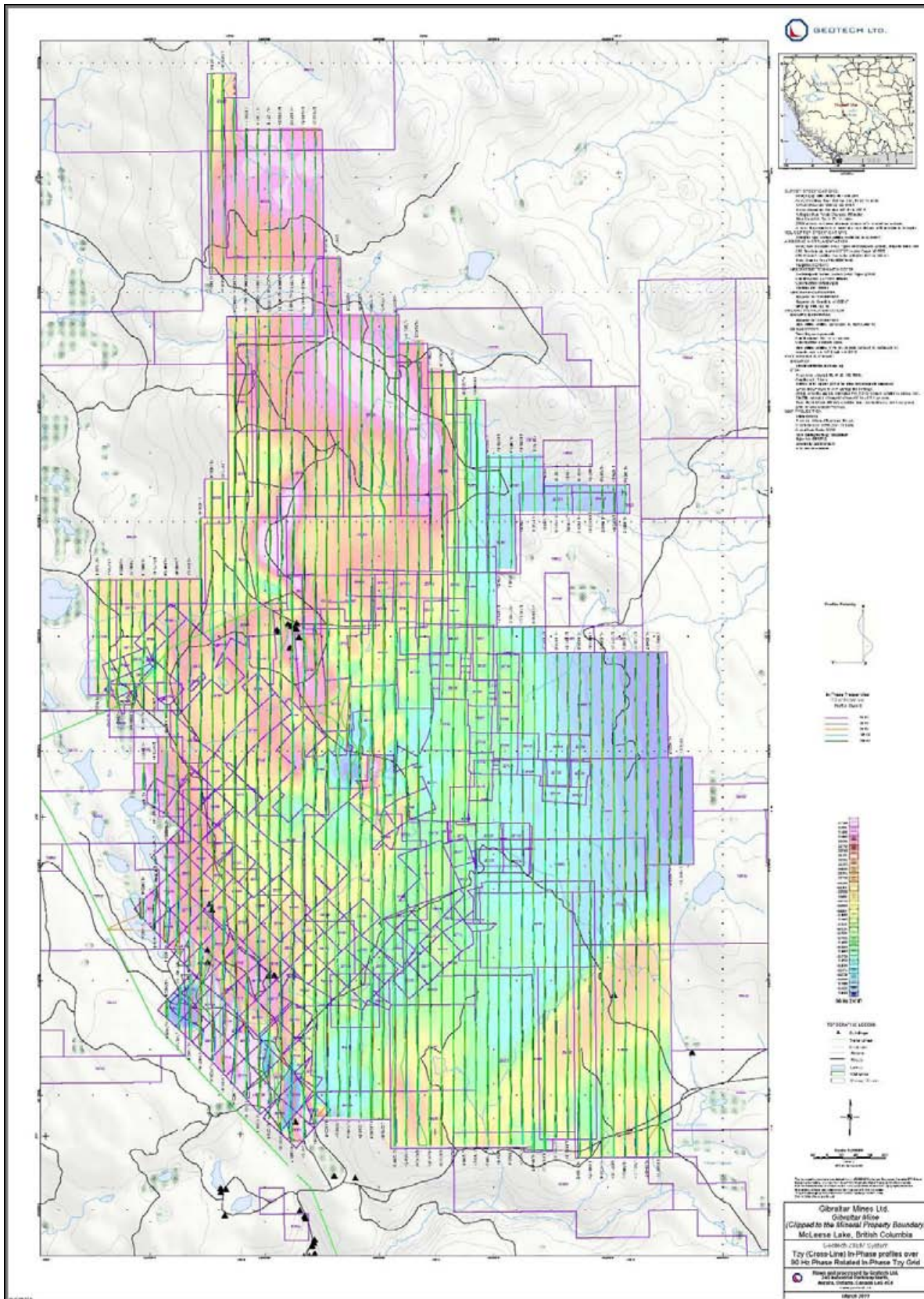
3D View of In-Phase, Total Phase Rotated (TPR) grids versus Skin Depth (30 Hz - 360 Hz) (Clipped)



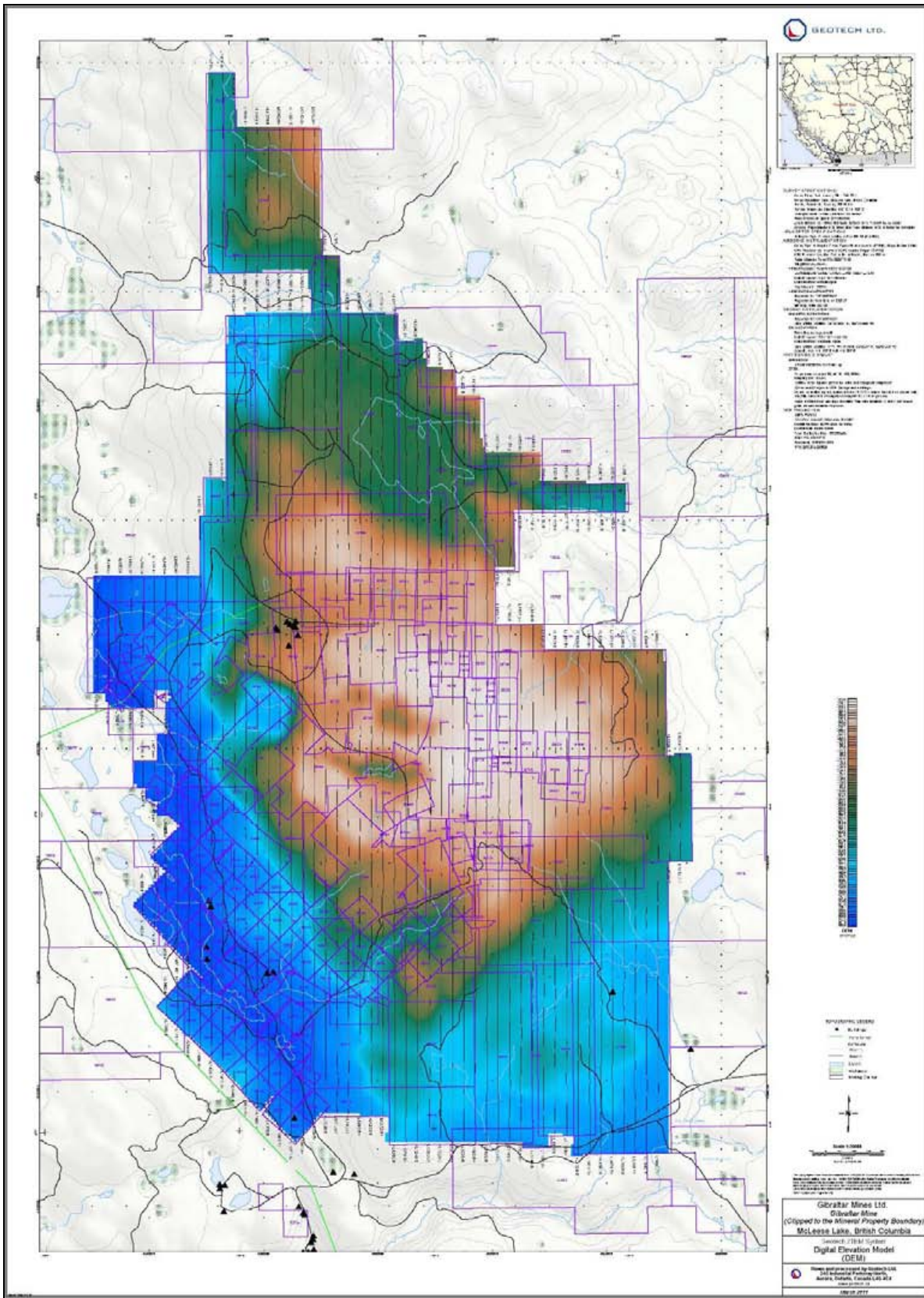
Tzx (In-Line) In-Phase Profiles over 90Hz Phase Rotated In-Phase Grid (Clipped)



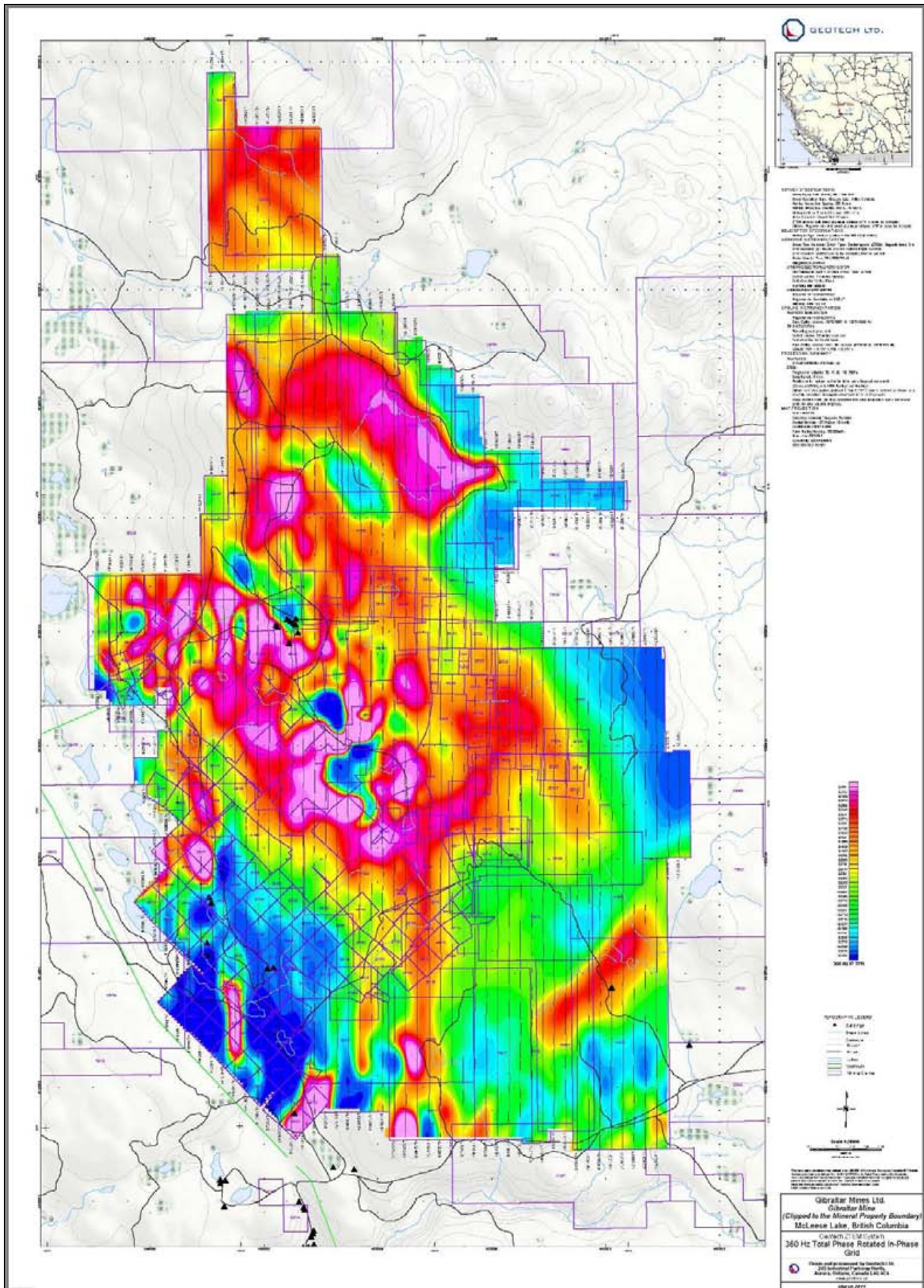
Tzx (In-Line) Quadrature Profiles over 90Hz Phase Rotated Quadrature Grid (Clipped)



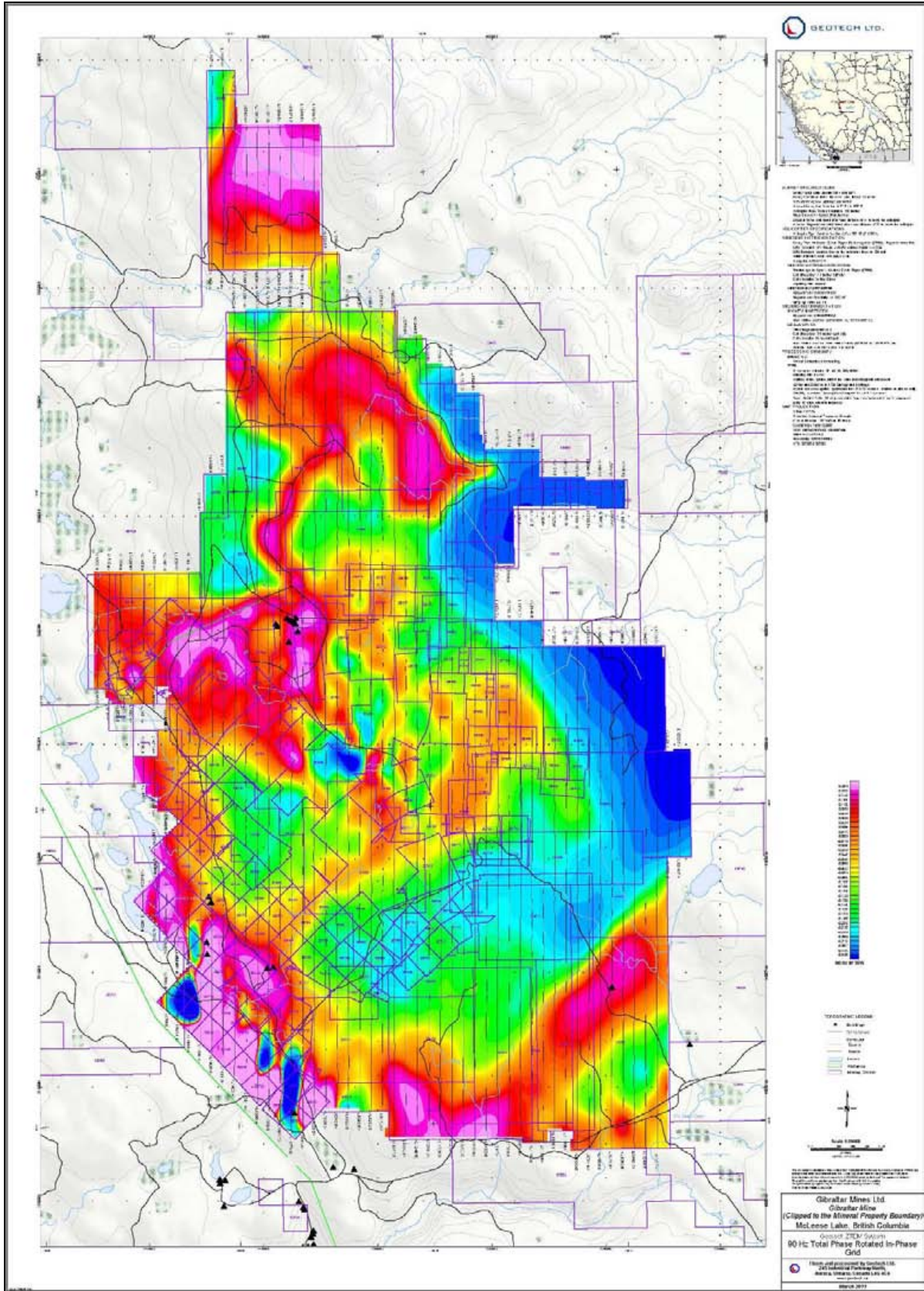
Tzy (Cross-Line) In-Phase Profiles over 90Hz Phase Rotated In-Phase Grid (Clipped)



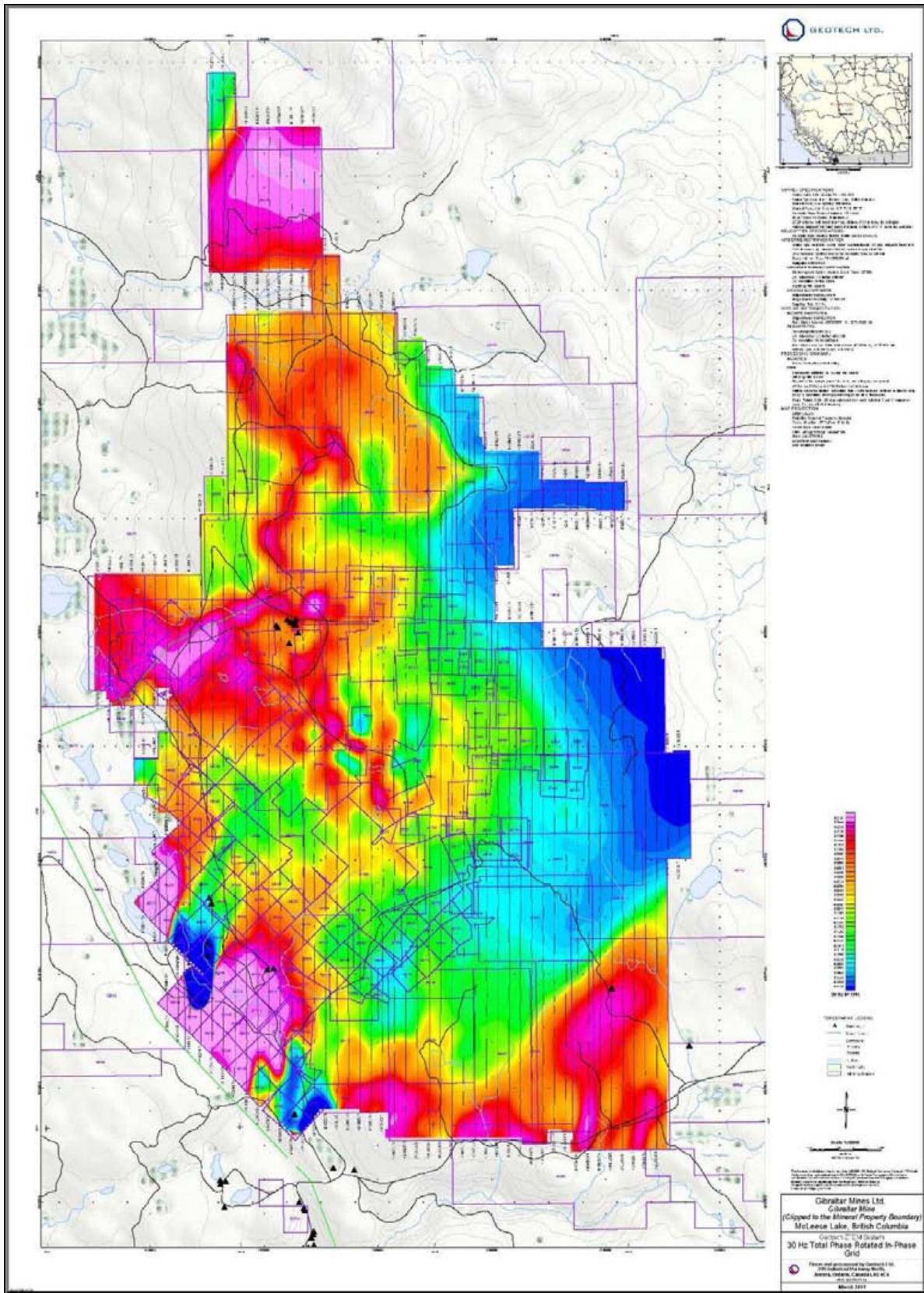
Digital Elevation Model (DEM)



High Frequency (360Hz) In-Phase Total Phase Rotated (TPR) (Clipped)



Mid Frequency (90Hz) In-Phase Total Phase Rotated (TPR) (Clipped)



Low Frequency (30Hz) In-Phase Total Phase Rotated (TPR) (Clipped)

APPENDIX D

ZTEM THEORETICAL CONSIDERATIONS

A brief section on the theory behind the AFMAG technique is provided for completeness and a more comprehensive development of the theory can be found in standard texts. The natural EM field is normally horizontally polarized. Subsurface lateral variations of conductivity generate a vertical component, which is linearly related to the horizontal field. Although the fields look like random signals, they may be treated as the sum of sinusoids. At each frequency the field can be expressed as a complex number with magnitude and argument equal to the amplitude and phase of the sinusoid. The relation between the field components can then be expressed by a linear complex equation with two complex coefficients at any one frequency. These coefficients are dependent upon the subsurface and not upon the horizontal field present at any particular time and are appropriate parameters to measure (Vozoff, 1972).

$$\mathbf{H}_z(\mathbf{f}) = \mathbf{T}_x(\mathbf{f}) \mathbf{H}_x(\mathbf{f}) + \mathbf{T}_y(\mathbf{f}) \mathbf{H}_y(\mathbf{f}), \quad (1)$$

Where

$\mathbf{H}_x(\mathbf{f})$, $\mathbf{H}_y(\mathbf{f})$ and $\mathbf{H}_z(\mathbf{f})$ are x, y and z components of the field,

$\mathbf{T}_x(\mathbf{f})$ and $\mathbf{T}_y(\mathbf{f})$ are the “tipper” coefficients.

In the case of a horizontally homogeneous environment, \mathbf{T}_x and \mathbf{T}_y are equal to zero because $\mathbf{H}_z = 0$. They show certain anomalies only by the presence of changes in subsurface conductivity in the horizontal direction. The real parts of the coefficients correspond to tangents of tilt angles measured with a controlled source. The complex tensor [\mathbf{T}_x , \mathbf{T}_y] known as the “tipper” defines the vertical response to horizontal fields in the x and y directions respectively.

\mathbf{T}_x and \mathbf{T}_y are two unknown coefficients in one equation, and we therefore must combine two or more sets of measurements to solve them. To reduce effects of noise, multiple sets of measurements can be made, and the coefficients, which minimize the squared error in predicting the measured Z from X and Y, can be found. This leads to next formulas for estimating the coefficients.

$$\mathbf{T}_x = ([\mathbf{H}_z\mathbf{H}_x^*] [\mathbf{H}_y\mathbf{H}_y^*] - [\mathbf{H}_z\mathbf{H}_y^*] [\mathbf{H}_y\mathbf{H}_x^*]) / ([\mathbf{H}_x\mathbf{H}_x^*] [\mathbf{H}_y\mathbf{H}_y^*] - [\mathbf{H}_x\mathbf{H}_y^*] [\mathbf{H}_y\mathbf{H}_x^*]), \quad (2)$$

and

$$\mathbf{T}_y = ([\mathbf{H}_z\mathbf{H}_y^*] [\mathbf{H}_x\mathbf{H}_x^*] - [\mathbf{H}_z\mathbf{H}_x^*] [\mathbf{H}_x\mathbf{H}_y^*]) / ([\mathbf{H}_x\mathbf{H}_x^*] [\mathbf{H}_y\mathbf{H}_y^*] - [\mathbf{H}_x\mathbf{H}_y^*] [\mathbf{H}_y\mathbf{H}_x^*]). \quad (3)$$

Where

[HxHy*] (For example) denotes a sum of the product of Hx with the complex conjugate of Hy.

In practical processing algorithms, all numbers Hx, Hy and Hz can be obtained by applying the same digital band-pass filters to three incoming parallel data signals. FFT algorithms are also applicable. All sums like [HxHy*] can be calculated on the basis of a discrete time interval in the range from 0.1 to 1 sec or on a sliding time base.

Using platform attitude data in the EM data processing can be done at different stages of the signal processing. The most obvious idea is to transform parallel data from local coordinates of the platform into absolute geographical coordinates before the main signal processing procedure. Unfortunately, the proper algorithms of attitude data obtained, often require some post-processing algorithms such as using post-calculated accelerations based on GPS data etc. That is why it is preferable to treat x-y-z coordinates in formulas above in the local coordinate system of the platform and to recalculate resulting local tilt angles into a geographical or global coordinate system later, during the data post processing.

In weak field conditions where the level of the signal is comparable with input noise levels in preamplifiers, the bias in the estimated values of Tx and Ty caused by noise in the horizontal signals become substantial and can not be reduced by any averaging. This bias can be removed by the use of separate reference signals containing noise uncorrelated with noise in signals Hx and Hy. (Anav et al., 1976).

$$T_x = ([H_z R_x^*] [H_y R_y^*] - [H_z R_y^*] [H_y R_x^*]) / ([H_x R_x^*] [H_y R_y^*] - [H_x R_y^*] [H_y R_x^*]), \quad (4)$$

and

$$T_y = ([H_z R_y^*] [H_x R_x^*] - [H_z R_x^*] [H_x R_y^*]) / ([H_x R_x^*] [H_y R_y^*] - [H_x R_y^*] [H_y R_x^*]). \quad (5)$$

Where:

Rx is the reference field x component,

Ry is the reference field y component.

An additional two electromagnetic sensors, providing these reference signals can be placed at some distance away from the main x, y and z sensors. Currently, though, no additional remote-reference processing are applied to ZTEM data.

Numerical Modelling

In order to understand the airborne AFMAG responses to conductors for a variety of geological environments, EMIGMATM modelling code from PetRos EiKon (Toronto, ON) was obtained to conduct the formulated model studies.

Below are some of the modelling results from their study.

Modelling assumption:

The assumptions for the modelling are that:

3 components of the magnetic field are measured and they are processed according to:

$$H_z(f) = T_x(f) H_x(f) + T_y(f) H_y(f)$$

The vector (Tx,Ty) is usually referred to as the ‘tipper’ vector and is determined in the frequency domain through processing. This is normally done by determining transfer functions from an extended time series.

For the modelling exercise, the 3 components of the magnetic vector (Hx,Hy,Hz) are modelled twice for 2 orthogonal polarizations of a plane wave source field and then the tipper is calculated from a matrix calculation using the results of the 2 source polarizations’ models. For the 2D forward modelling results, the tipper vectors are shown as a function of frequency

Basic Model Response

For the initial models, we assume a thin plate-like model. The model is perpendicular to the flight direction. Initially, we will assume very long strike directions. From this quasi-2D model, there are 2 basic responses. The so-called TE response and the so-called TM response.

For the initial models, we will assume the strike is in the y (North) directions and the flight is in the x (East) direction. Sensor heights are 30m above ground.

TE Mode: For the TE response, the electric field excitation flows along strike (current channelling) and the horizontal H field (Hx) flows perpendicular to strike thus causing induction through Faraday’s law. The Hz response is generated both from channelling and induction.

TM Mode: For this response, the electric field excitation flows perpendicular to strike generating quasi-static charges on faces and the horizontal H field (Hx) flows parallel to strike. Since, the XZ face is very small for this model, little current is induced. The charges on the faces have a small dipole moment due to the thinness of the model.

For the rest of the models unless otherwise noted, the parameters used are:

Strike Length: 1km

Depth Extent: 1km

Conductance: 100S

Depth to Top: 10m

Background: Thin-overburden (10m), Resistive Basement (1000 Ohm-m)

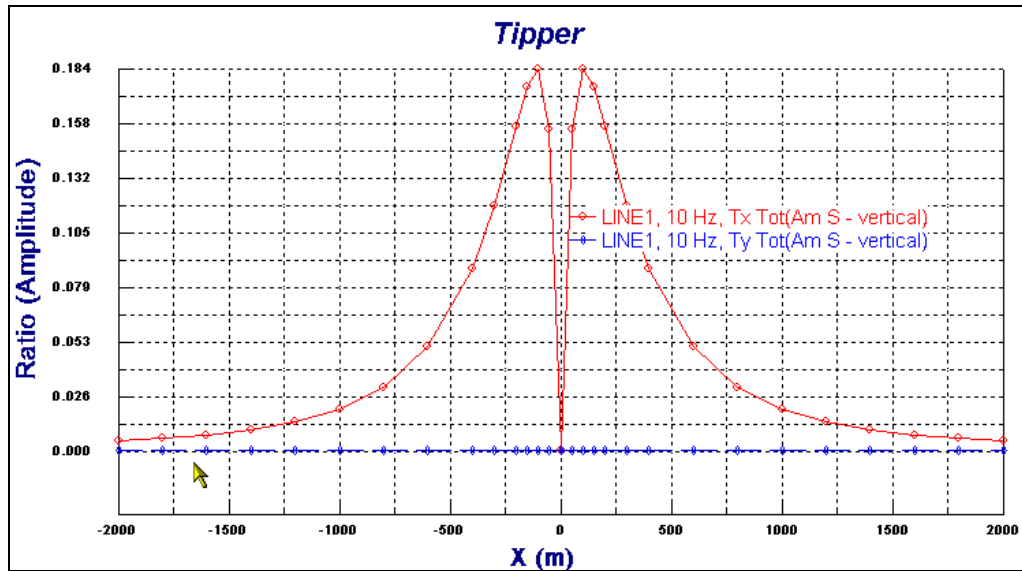


Figure D-1 – Calculated Tipper components at 10 Hz for above model parameters.

Figure D1 shows the Tipper (Tx,Ty) Amplitudes at 10Hz using a 10Ωm overburden. Note small Ty (ie quasi-TM response)

Amplitude Response

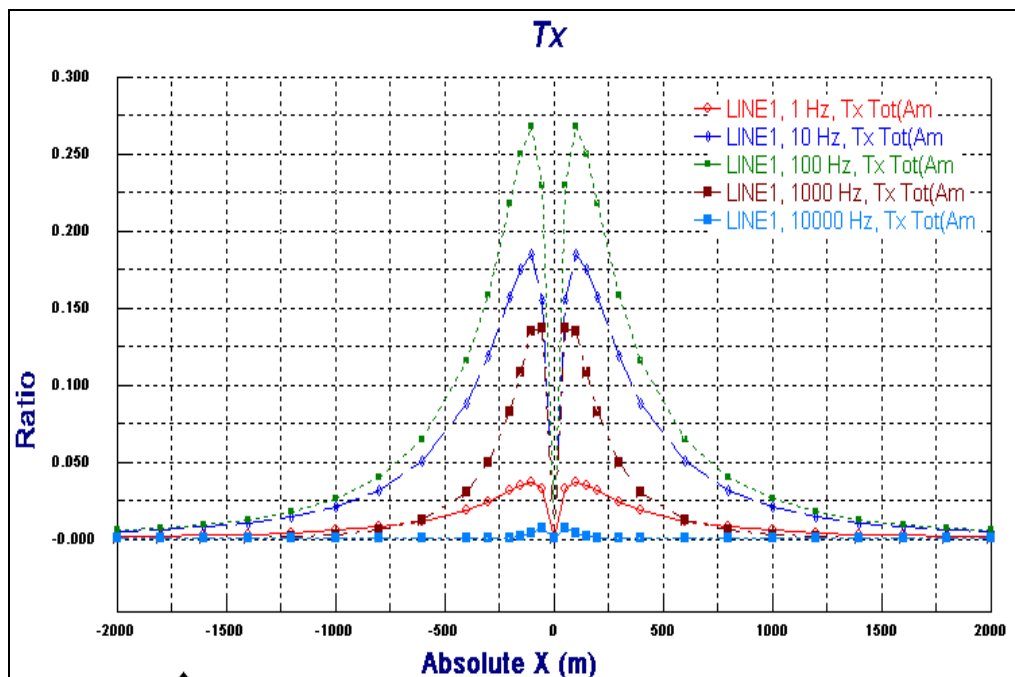


Figure D-2 – Calculated Tx component of the Tipper at various frequencies

The (Tx) response amplitude at 1,10,100,1000,10000 Hz. Peak amplitude at 100Hz

Inphase and Quadrature Response

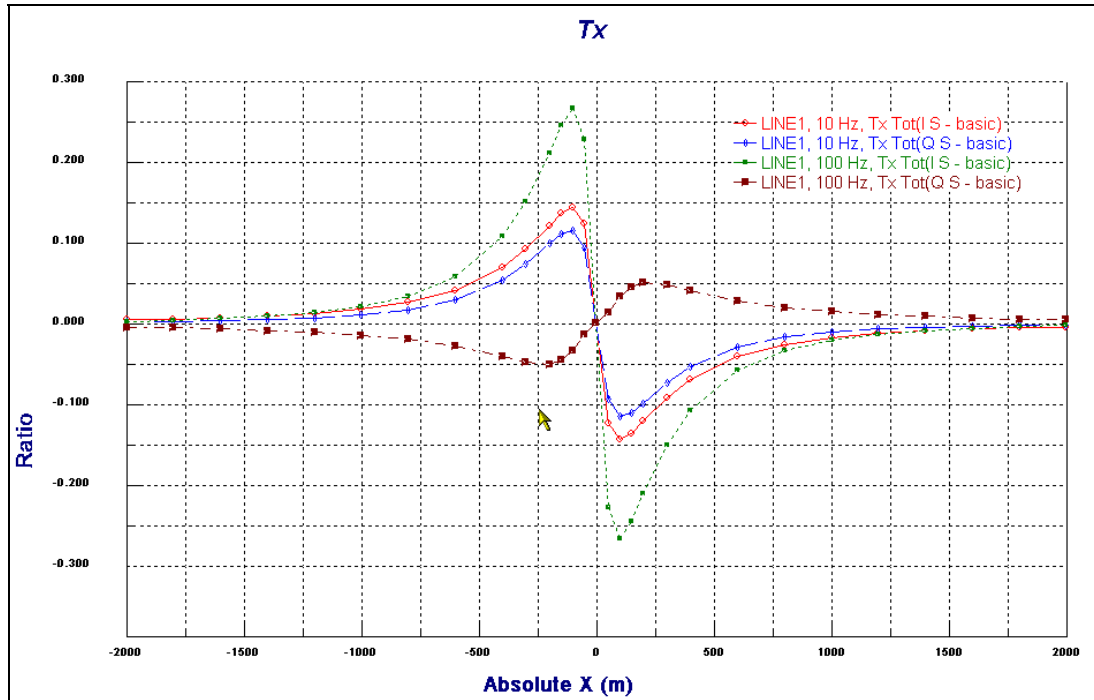


Figure D-3 – Calculated In-phase and Quadrature of the Tx component at various frequencies

Figure D-3 shows the In-phase and Quadrature response at 10 and 100Hz. Note the crossovers in the In-phase and Quadrature, and the phase reversal in the Quadrature responses from low to high frequencies.

Bo Lo, P.Eng, B.Sc. (Geophysics), Consultant
Geotech Ltd.
September, 2007

AFMAG Source Fields and ZTEM method¹

AFMAG uses naturally occurring audio frequency magnetic fields as the source of the primary field signal, and therefore requires no transmitter (Ward, 1959). The primary fields resemble those from VLF except that they are lower frequency (tens & hundreds of Hz versus tens of kHz) and are usually not as strongly directionally polarized (Labson et al., 1985). These EM fields used in AFMAG are derived from world wide atmospheric thunderstorm activity, have the unique characteristic of being uniform, planar and horizontal, and also propagate vertically into the earth – to great depth, up to several km, as determined by the magnetotelluric (MT) skin depth (Vozoff, 1972), which is directly proportional to the ratio of the bedrock resistivity to the frequency (Figure D4).

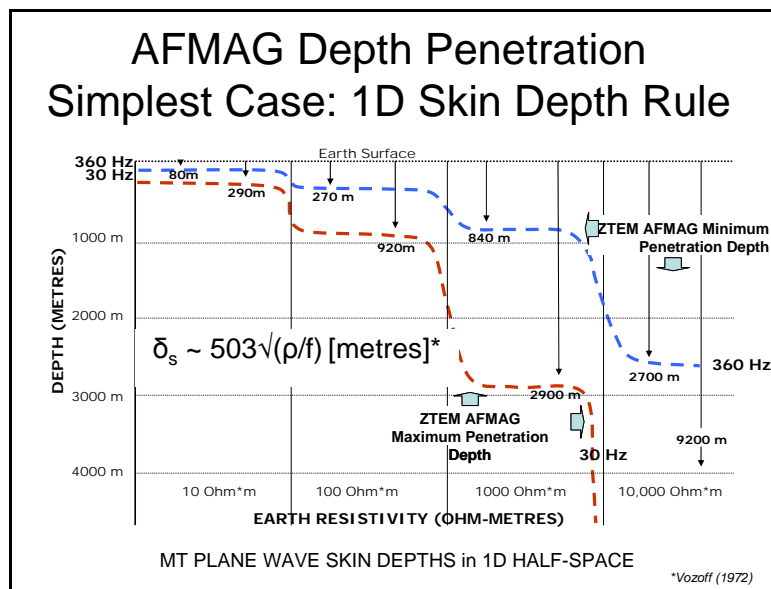


Figure D4: MT Skin Depth Penetrations for ZTEM in 30-360Hz and 10-1000 ohm resistivity

At the frequencies used for ZTEM, the penetration depths likely range between approx. 600m to 2km in this region (approx. 1k ohm-m avg. resistivity assumed), according to the following equation for the Bostick skin depth $\delta_B = 356 * \sqrt{(\rho / f)}$ metres (Bostick, 1977), which is considered appropriate as a rule of thumb equivalent depth estimate.

The other unique aspect of AFMAG fields is that they react to relative contrasts in the resistivity, and therefore do not depend on the absolute conductance, as measured using inductive EM systems, such as VTEM. Hence poorly, conductive targets, such as alteration zones and fault zones can be mapped, as well as higher conductance features, like graphitic units. Conversely, resistive targets can also be detected using AFMAG– provided they are of a sufficient size and contrast to produce a vertical field anomaly. Indeed resistors produce reversed anomalies relative to conductive features. Hence AFMAG can be effective as an

¹From: Legault, J.M., Kumar, H., and Milicevic, B. (2009): ZTEM tipper AFMAG and 2D inversion results over an unconformity uranium target in northern Saskatchewan, Expanded Abstract submitted to Society of Exploration Geophysics SEG conference, Houston, Tx, Nov-2009, 5 pp.

all-round resistivity mapping tool, making it unique among airborne EM methods. A series of 2D synthetic models that illustrate these aspects have been created using the 2D forward MT modelling code of Wannamaker et al. (1987) and are presented in figures D5-D7.

The tipper from a single site contains information on the dimensionality of the subsurface (Pedersen, 1998), for example, in a horizontally stratified or 1D earth, $T=0$ and as such H_Z is absent. For a 2D earth with the y -axis along strike, $T_Y=0$ and $H_Z = T_X * H_X$. In 3D earths, both T_X and T_Y will be non-zero. H_Z is therefore only present, as a secondary field, due to a lateral resistivity contrast, whereas the horizontal H_X and H_Y fields are a mixture of secondary and primary fields (Stodt et al., 1981). But, as an approximation, as in the telluric-magnetotelluric method (T-MT; Hermance and Thayer, 1975) used by distributed MT acquisition systems, the horizontal fields are assumed to be practically uniform, which is particularly useful for rapid reconnaissance mapping purposes. By measuring the vertical magnetic field H_X , using a mobile receiver and the orthogonal horizontal H_X and H_Y fields at a fixed base station reference site, ZTEM is a direct adaptation of this technique for airborne AFMAG surveying.

Jean M. Legault, M.Sc.A., P.Eng., P.Geo.
Geotech Ltd.

References

- Bostick, F.X., 1977, A simple almost exact method of MT analysis. Proceedings of the University of Utah Workshop on Electrical methods in Geothermal Exploration, 175-188.
- Hermance, J.F., and Thayer, R.E., 1975, The telluric-magnetotelluric method, *Geophysics*, **37**, 349-364.
- Labson, V. F., A. Becker, H. F. Morrison, and U. Conti, 1985, Geophysical exploration with audio-frequency natural magnetic fields: *Geophysics*, **50**, 656–664.
- Murakami, Y., 1985, Short Note: Two representations of the magnetotelluric sounding survey, *Geophysics*, **50**, 161-164.
- Pedersen, L.B., 1998, Tensor VLF measurements: Our first experiences, *Exploration Geophysics*, **29**, 52-57.
- Stodt, J.A., Hohmann, G.W., and Ting, S.C., 1981, The telluric-magnetotelluric method in two- and three-dimensional environments, *Geophysics*, **46**, 1137-1147.
- Vozoff, K., 1972, The magnetotelluric method in the exploration of sedimentary basins, *Geophysics*, **37**, 98–141.
- Ward, S. H., 1959, AFMAG—Airborne and ground: *Geophysics*, **24**, 761–787.
- Wannamaker, P.E., Stodt, J.A., and Rijo, L., 1987, A stable finite element solution for two-dimensional magnetotelluric modelling, *Geophy. J. Roy. Astr. Soc.*, **88**, 227-296.

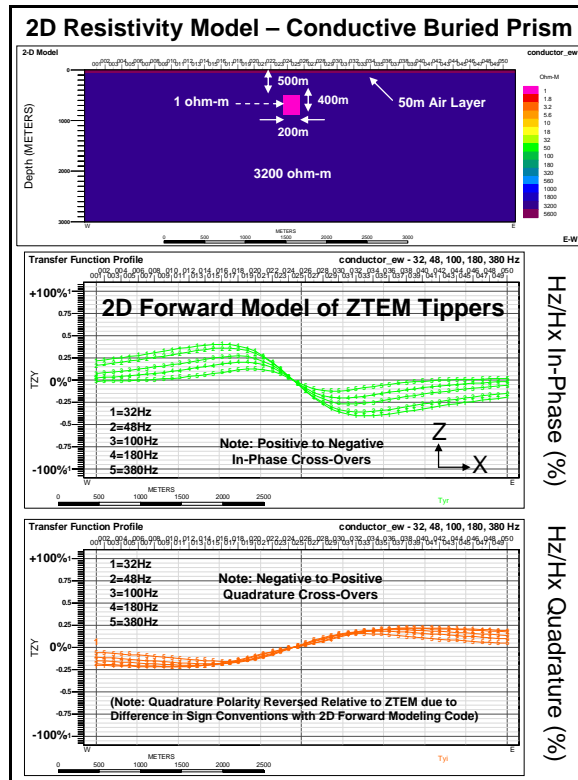


Figure D5: 2D synthetic forward model Tipper responses (Tzy) for conductive brick model.

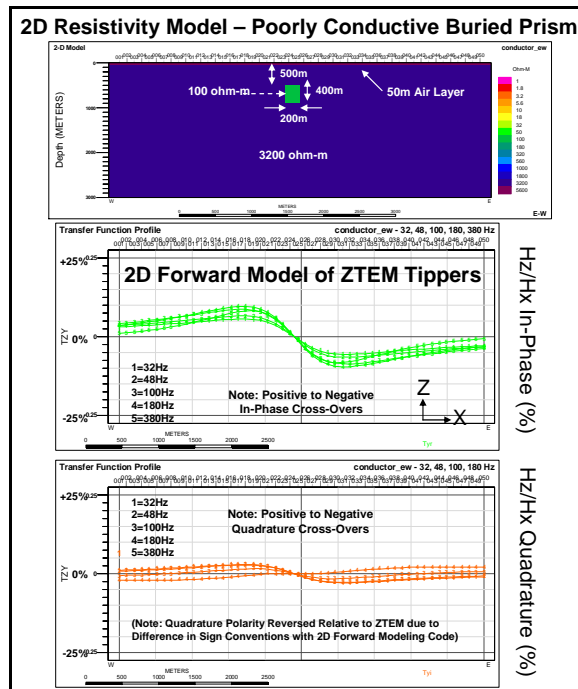


Figure D6: 2D synthetic forward model Tipper response (Tzx) for poorly conductive brick model.

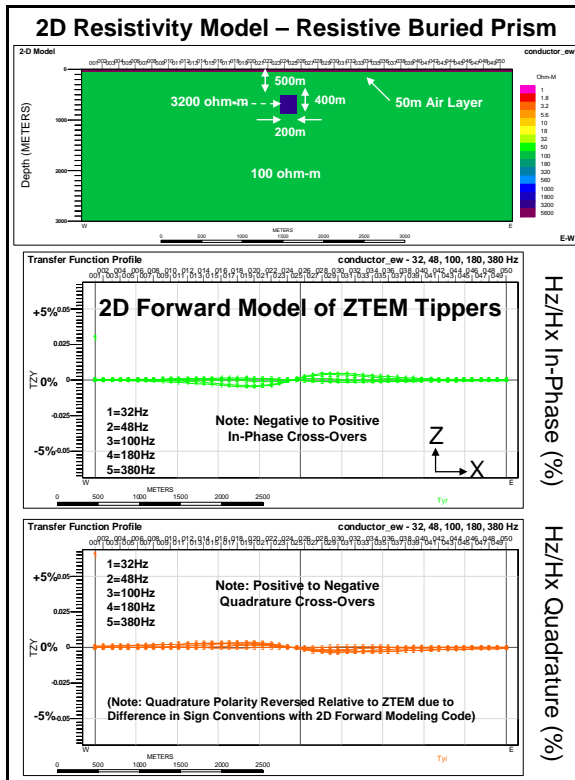


Figure D7: 2D synthetic forward model Tipper response (T_{zx}) for resistive brick model.

APPENDIX E

ZTEM (AIRBORNE AFMAG) TESTS OVER UNCONFORMITY URANIUM DEPOSITS⁴

Bob Lo¹, Jean Legault², Petr Kuzmin³ Formerly Geo Equipment Manufacturing Ltd., now Exploration Syndicate, Inc., bob.lo@expsyn.com, Geotech Ltd., jean@geotech.ca, Geo Equipment Manufacturing Ltd., petr@geotech.ca*

Key Words: ZTEM, AFMAG, electromagnetic, airborne, uranium, Athabasca.

INTRODUCTION

A series of demonstration tests were conducted using the ZTEM, airborne AFMAG system over deep targets in the Athabasca Basin of Saskatchewan, Canada. These tests were conducted in mid-2008 and were flown to test ZTEM's ability to detect large conductive targets at depth; deeper than conventional airborne EM methods. Data are presented over areas where the conductors are located 450-600 metres beneath the surface. As well, a case of ZTEM following the plunge of a conductor to over 800 metres depth is shown.

BACKGROUND

The ZTEM system is the latest implementation of an airborne AFMAG system first commercialized in late 2006. ZTEM uses a large, 8 metre diameter airborne air core coil, slung from a helicopter, to measure the vertical component of the AFMAG signal. Two 4 metre square coils are deployed on the ground to measure the horizontal field. The ZTEM system has flown successful demonstration surveys over porphyry copper deposits in the southwest USA (Zang et al., 2008).

ZTEM was tested in the Athabasca Basin in Canada in May of 2008 to determine its depth of investigation and to determine its suitability for mapping deep conductors in the crystalline basement. Over 30% of the world's U3O8 is mined in the Athabasca Basin from unconformity uranium deposits. Unconformity uranium deposits of the Athabasca Basin are often associated with conductors located in the crystalline basement. The search for economic uranium deposits is moving to areas of the basin which are deeper and beyond the detection limits of modern airborne instrumentation. This creates the requirement for a system which can detect conductivity past the detection limits of modern traditional EM systems. This was the motivation behind the field trials of the ZTEM system in the Athabasca Basin. Several areas where known deep conductors (450-600m+) were located were flown. Also, a test survey block in the northern part of the basin was able to trace a deep and plunging conductor to depths that no other airborne EM system has been able to achieve.

ATHABASCA BASIN GEOLOGY

The high-grade uranium deposits within the Athabasca Basin are associated with the unconformity between the essentially flat-lying Proterozoic Athabasca Group sandstones and the underlying Archean-Paleoproterozoic metamorphic and igneous basement rocks. The deposits occupy a range of positions from wholly basement-hosted to wholly sediment-hosted, at structurally favourable sites in the interface between the deeply weathered basement and overlying sediments of the Athabasca Basin (Ruzicka, 1997). The locations of These deposits are lithologically and structurally controlled by the sub-Athabasca unconformity and basement faults and fracture zones, which are localized in graphitic pelitic gneisses that may flank structurally competent Archean granitoid domes (Quirt, 1989).

In general, most of the known important deposits tend to occur within a few tens to a few hundred metres of the unconformity and within 500 m of the current ground surface. This may be more of a limitation of exploration techniques. There is no reason to believe that the distribution of the deposits is dependent on the modern day depth of

⁴ Extended abstract submitted to 20th ASEG International Geophysical Conference & Exhibition, Adelaide, AU, 22-26 Feb, 2009.

burial.

Empirically, the geophysical exploration for unconformity type uranium targets have been to search for large basement structures which post date the sandstone deposition of the basement (Matthews et. al, 1997). All the deposits located so far are associated with fault structures associated with a graphitic conductive basement. An alteration zone of clay silicification and enrichment around the deposits probably leads to magnetite destruction causing the magnetic low observed around the deposits. The clay alteration should give rise to a resistivity low signature about the deposits. The low conductivity of the clay alteration makes it a difficult target for airborne EM if it is buried at significant depth.

ZTEM INSTRUMENTATION AND PRESENTATION

ZTEM is an airborne AFMAG system introduced by Geotech Ltd. of Canada in early 2007 (Lo et al., 2008). In a ZTEM survey, a single vertical dipole air-core coil is flown over the survey area in a grid pattern similar to other airborne electromagnetic surveys. Two orthogonal, air-core, horizontal axis coils placed close to the survey site measures the horizontal EM fields for reference. A GPS array on the airborne coil monitors its attitude for post-flight corrections.

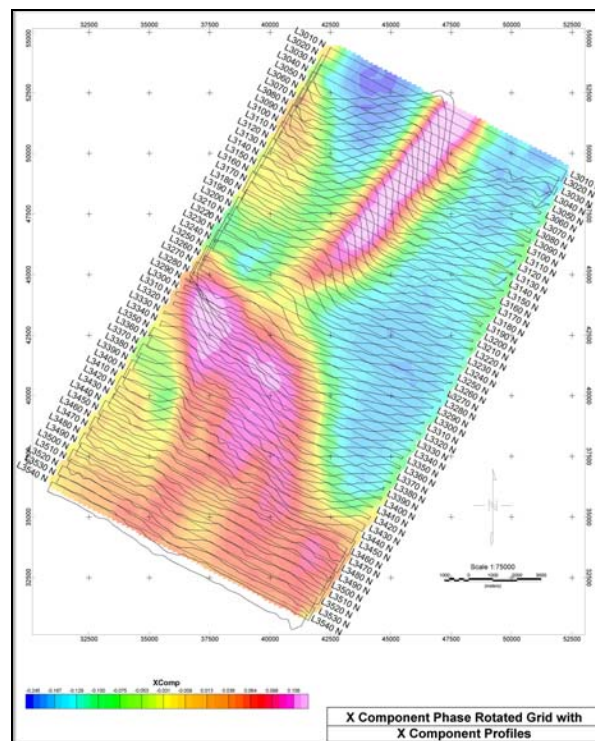


Figure 1 – Stacked profiles of the x-component Tipper over the gridded values of the phase rotated x-component data. Note that the cross-overs in the profiles are now peaks on the image.

As the source field is assumed to be far away, the excitation of the ground is more or less uniform. For large structures, the signal fall-off will be much slower than from a dipole source, such as those energized by traditional airborne systems. With the ZTEM system being less susceptible to terrain clearance, the planned ground clearance height is higher and the terrain drape is looser as compared to standard helicopter EM surveys.

The two Tippers obtained from the relationship between the vertical airborne coil and the two ground coils have a cross-over over a steeply dipping, plate-like body. The cross-overs can be made into local maxima via a 90 degree phase rotation which allows for easier interpretation of the gridded values. Figure 1 is an example of this transformation.

To present the data of both Tippers as one image, we calculate a parameter termed the DT which is the horizontal divergence of the two Tippers, much in the same manner as the “peaker” parameter in VLF (Pedersen, 1998). The DT is typically plotted with an inverted colour bar as it is negative over a steeply dipping thin body.

ZTEM RESULTS – NORTHERN ATHABASCA BASIN

Figure 2 shows gridded values from a number of ZTEM lines over an area where the sedimentary cover is approximately 450-600 metres thick. A number of traditional EM systems have also been flown over this block. While they were able to detect conductors, the resolution of the conductive features is not nearly as detailed as the information provided by ZTEM.

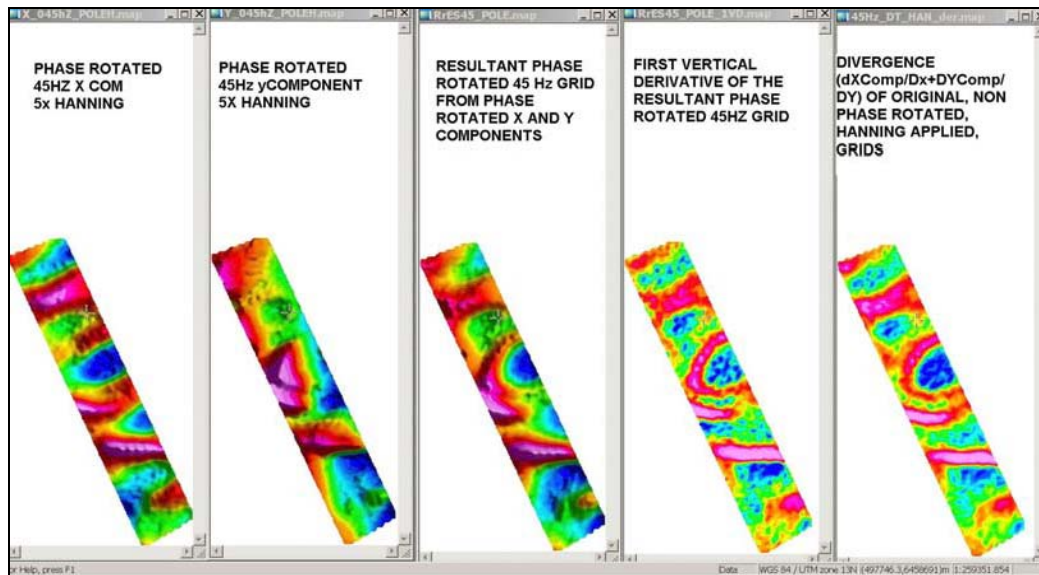


Figure 2 – ZTEM results over an area of 450-600 metre thick sedimentary cover.

Figure 3, from another area, shows the data from one of the larger blocks that was flown. It is a 3D composite image of the DT at various frequencies plotted at the equivalent skin depth assuming a 1,000 ohm-m average resistivity.

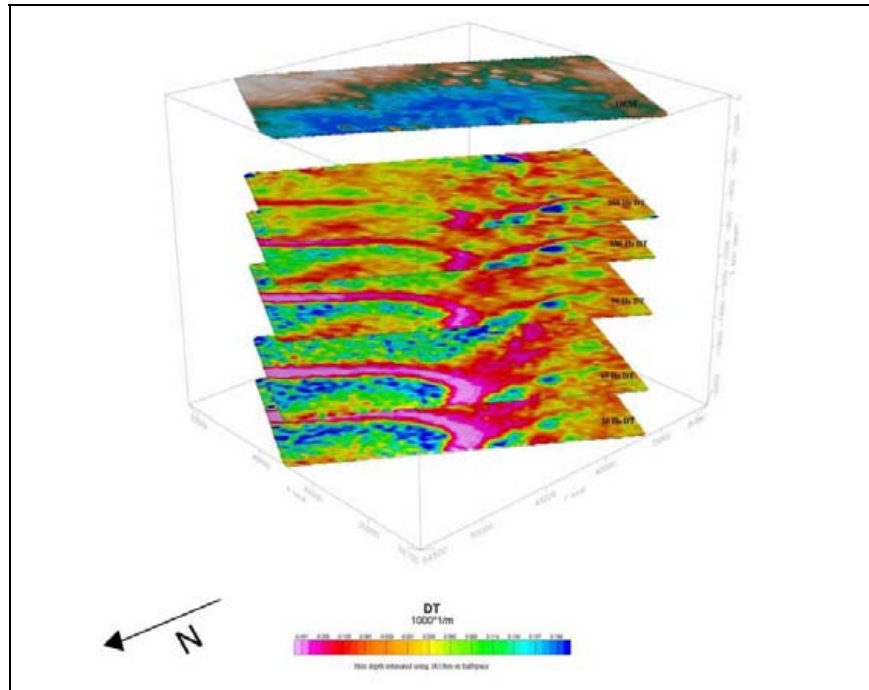


Figure 3 - Perspective view of DT's of different frequencies plotted at the skin depth (using a 1,000 ohm-m Earth).

The data in Figure 3 come from a survey over the north rim of the Athabasca Basin. The sandstone cover is about 500m on the left hand side of the image, and progressively getting deeper to the right. It is about 700m in the middle part of the image and over 800 metres thick on the right middle portion where exploration drilling is concentrated. Starting in the middle left and trending to the right of the image, there is a known graphitic shear.

In the uppermost (600m) “depth slice”, Figure 3 shows a linear conductive feature that progressively weakens as one moves to the right until it is no longer seen. This is interpreted to be due to the graphitic shear conductor plunging deeper past the depth of investigation of the 360 Hz data. The lower frequencies penetrate more into the sedimentary cover that is deeper towards the right. DT's of decreasing frequency show the linear conductive feature extending more and more to the right. The feature also strengthens/sharpens into a synformal shape with lower frequencies. This fits with what the known geology of a plunging conductor at depth is doing.

At the nose of the fold, in the right third of the images, we also see another, broader anomalous zone that trends towards the back of the image. At this location, two radioactive springs are situated. These spring waters which are anomalously high in uranium and radon may reflect the upward migration of deep waters along faults, suggesting structural targets in areas where basinal waters may have tapped a radioactive source. This broad DT trend might be the plunge of the fold axis that is aligned away from the front of the image. An anomaly along this trend, at the highest frequency, that steadily grows with each decreasing frequency can be seen. This might represent an alteration zone in the sandstone that is detected at the shallowest depth. By about the 90Hz DT depth slice or so, we are possibly in the deeper basement and into a basement graphitic unit.

CONCLUSIONS

A number of successful ZTEM tests were conducted over the Athabasca Basin. The tests demonstrated that ZTEM can easily detect conductivity to 800 metres beneath relatively resistive sedimentary cover. Assuming a 1,000 ohm-metre

resistivity, the skin depth of the 30 Hz data is approximately 2,000 metres. The 30 Hz data presented have good signal to noise ratios indicating a deep depth of exploration. The observation that ZTEM may be detecting the clay alteration above the crystalline basement is a significant advantage for exploration of unconformity uranium deposits.

More demonstration surveys are planned in the Athabasca Basin later this year. And more target types for testing are also planned.

ACKNOWLEDGEMENTS

The authors thank Geotech Ltd. for allowing them to publish this work and for providing the support required to write this abstract and to present this paper.

REFERENCES

- Labson, V. F., Becker A., Morrison, H. F., and Conti, U., 1985, Geophysical exploration with audiofrequency natural magnetic fields, *Geophysics*, Vol. 50, p. 656-664.
- Lo, B., Zang, M., Kuzmin, P., 2008, Geotech's Z-TEM (Airborne AFMAG) Instrumentation, a paper presented at KEGS PDAC 2008 Symposium, Toronto.
- Matthews, R., Koch, R. and Leppin, M., 1997, Advances in Integrated Exploration for Unconformity Uranium Deposits in Western Canada; in *Proceeding of Exploration 97*, edited by Arnis Gubins, Prospectors and Developers Association of Canada, Toronto.
- McMullan, S.R., Matthews, R.B, and Robertshaw, P., 1990, Exploration geophysics for Athabasca Uranium Deposits, in: *Proceedings of Exploration 87*, Ontario Geological Survey.
- Pedersen, L.B, Qian, W., Dynesius, L., Zhang, P., 1994, An airborne tensor VLF system. From concept to realization, *Geophysical Prospecting*, Vol. 42.
- Ruzicka, V.R., 1997, Metallogenic features of the uranium-polymetallic mineralization of the Athabasca Basin, Alberta, and a comparison with other parts of the basin; in R.W. Macqueen, ed., *Geological Survey of Canada, Bulletin 500*, 31-79.
- Wheatley, K., Murphy, J., Leppin, M., and Climie, J.A., 1996, Advances in the Genetic Model and Exploration Techniques for Unconformity-type Uranium Deposits in the Athabasca Basin; in Ashton, K.E., Harper, C.T., eds., *MinExpo '96 Symposium – Advances in Saskatchewan Geology and Mineral Exploration: Saskatchewan Geological Society, Special Publication No 14*, p. 126-136.
- Quirt, D., 1989, Host rock alteration at Eagle Point South: Sask. Research Council, Publication no. R-855-1-E- 89, 95p.
- Ward, S. H., 1959, AFMAG - Airborne and Ground: *Geophysics*, Vol. 24, p. 761-787.
- Zang, M., Lo, B., 2008, The Application of Airborne Natural Field Electromagnetics (ZTEM): Some Examples from the Southwestern United States, a paper presented at the 2008 PDAC, Toronto